

NACA RM E53G01

SEP 15 1953



RESEARCH MEMORANDUM

INVESTIGATION OF LOW-PRESSURE PERFORMANCE OF
EXPERIMENTAL TUBULAR COMBUSTORS DIFFERING
IN AIR-ENTRY-HOLE GEOMETRY

By Ralph T. Dittrich

Lewis Flight Propulsion Laboratory
Cleveland, Ohio

CLASSIFICATION CHANGED
UNCLASSIFIED

To

NACA LIBRARY

By authority of

Mason PA 3 Effective Date 12-3-58
NB 3-2-59

LANGLEY AERONAUTICAL LABORATORY
Hampton Field, VA

CLASSIFIED DOCUMENT

This material contains information affecting the National Defense of the United States within the meaning of the espionage laws, Title 18, U.S.C., Secs. 793 and 794, the transmission or revelation of which in any manner to an unauthorized person is prohibited by law.

NATIONAL ADVISORY COMMITTEE FOR AERONAUTICS

WASHINGTON

September 4, 1953

CONFIDENTIAL

UNCLASSIFIED



3 1176 01435 2661

NATIONAL ADVISORY COMMITTEE FOR AERONAUTICS

RESEARCH MEMORANDUM

INVESTIGATION OF LOW-PRESSURE PERFORMANCE OF EXPERIMENTAL TUBULAR
 COMBUSTORS DIFFERING IN AIR-ENTRY-HOLE GEOMETRY

By Ralph T. Dittrich

SUMMARY

An investigation was conducted to determine, by experiments within the scope of air-entry-hole geometry, design criteria for tubular combustors having good low-pressure performance. Combustion efficiency, operable fuel-air-ratio and pressure ranges, and minimum ignition pressures were determined for numerous 6.25-inch-diameter combustor configurations at conditions simulating a 5.2-pressure-ratio turbojet engine operating at 85 percent of rated rotor speed, a flight Mach number of 0.6, and altitudes from 56,000 to 80,000 feet.

The best over-all performance with respect to combustion efficiency, operable fuel-air-ratio and pressure ranges, exhaust-gas temperature profile, and combustor-wall temperatures was obtained with combustor configurations having alternate zones of closely spaced 1/16-inch-diameter holes and widely spaced 5/8-inch-diameter holes throughout most of the combustor length. The maximum combustion efficiencies obtained for a temperature rise of 680° F were 94, 85, and 67 percent at simulated altitudes of 56,000, 70,000, and 80,000 feet, respectively. With a configuration having an ignition and flame-piloting region located upstream of the normal fuel-spray cone, ignition was obtained at a pressure of 3.8 inches of mercury absolute and an air-flow rate of 0.93 pound per second per square foot by means of an inductance spark having an estimated energy of 0.025 joule per spark.

INTRODUCTION

Combustion research in progress at the NACA Lewis laboratory includes studies of design criteria for turbojet combustors. The research described herein consists of preliminary investigations of the effects of air-entry-hole geometry on the low-pressure performance of a tubular, research combustor.

In the operation of current turbojet engine combustors at low inlet-air-pressure conditions, high altitude and low engine speed, the following combustor operational deficiencies are encountered: (1) low combustion efficiency, (2) flame blow-out and instability, (3) insufficient temperature rise, and (4) nonignition. Previous investigations, some of which are summarized in reference 1, indicate the existence of a relation between combustor air-entry-hole geometry and low-pressure performance.

The investigation described herein had a two-fold objective: (1) to determine, by experiments within the scope of air-entry-hole geometry, design criteria for tubular combustors having good low-pressure performance and (2) to achieve a better understanding of the relation between air-entry-hole geometry and combustor performance at low-pressure operating conditions. The air-entry-hole geometries investigated included variations in hole size, total hole area, hole-area distribution, and hole arrangement. Hole arrangement was varied to induce different air-flow patterns within the combustion zone.

A total of 104 different combustor-liner configurations of 6.25-inch diameter were tested in a relatively large-diameter test chamber. A large-diameter test chamber was used in place of a conventional close-fitting combustor housing in order to provide equal static pressures at all air-entry holes for all configurations. The performance of each configuration was determined on the basis of combustion efficiency, flame blow-out, and ignition, at inlet-air pressures of 15, 8, and 5 inches of mercury absolute, an inlet-air temperature of 268° F, and air-flow rates representative of current engine-design practice. These inlet-air conditions simulated operation of a 5.2-pressure-ratio engine at a flight Mach number of 0.6 and altitudes from 56,000 to 80,000 feet. The relatively low-pressure-ratio engine was considered because it entails more difficult combustion conditions. Fuel conforming to specification MIL-F-5624A grade JP-4 was used in the investigation.

The results presented herein are for 55 selected configurations that (1) gave the best performance or (2) best illustrate the trends observed. A discussion of the observed effects of alterations in air-entry-hole geometry on combustor performance is presented. In addition, the performance trends of several experimental configurations are compared with those of a current production-model turbojet combustor.

APPARATUS

Test Installation

A diagram of the test-chamber installation is shown in figure 1. The air-supply and exhaust ducts were connected to the laboratory combustion-air and low-pressure-exhaust systems, respectively. Air-flow

rates and chamber pressures were regulated by means of suitable remote-control valves. An electric air heater supplied the necessary preheated air.

Test Chamber

A relatively large-diameter test chamber (24-in. diam., 30-in. length), details of which are shown in figure 1, was used in order to maintain equal static-pressures at all air-entry-holes for all configurations. The combustor unit was accessible and removable through an 18-inch-diameter manhole. By means of observation windows located in the manhole and in the T-section of the combustor exhaust (fig. 1), both side and axial views of the flame were possible. Side views of the flame were obtained by sighting through the liner air-entry holes.

As shown in detail A, figure 1, the plate that served as the upstream enclosure for the combustor and on which were mounted the fuel atomizer and the ignition plug had a 6.25-inch-diameter V-groove on its downstream face. A ring at the exhaust end of the combustor (detail B, fig. 1) had a similar V-groove on its upstream face. The combustor liner, assembled between the plate and the ring, had its ends located in the V-grooves. Three clamp rods, equally spaced in a 7.25-inch-diameter circle, were connected by removable pins to a bracket assembly that was anchored to the downstream wall of the test chamber. At the upstream end of the combustor the rods fitted loosely into the holes of the plate (detail A) and were provided with coil springs and adjustment nuts. The use of coil springs prevented damage to the combustor assembly by thermal expansion. An adjustable vertical support (not shown) was located under the combustor end plate in order to prevent sagging of the combustor assembly. A small pipe (fig. 1) connecting the low point of the test chamber with the low-pressure-exhaust duct was used to drain-off any liquid fuel that might accumulate in the test chamber during the starting procedure.

Instrumentation

Air flow to the combustors was metered by a sharp-edged orifice (fig. 1) installed according to A.S.M.E. specifications; fuel flow was metered by a calibrated rotameter. The combustor inlet-air temperature was measured by means of a single iron-constantan thermocouple located at station 1 (fig. 1). Exhaust-gas temperatures were measured at station 3 by means of 17 chromel-alumel thermocouples. Details of thermocouple construction and arrangement are given in figure 2. The temperature of the thermocouple located on the duct center line at station 3

was used for reference only. The temperatures measured by the remaining 16 thermocouples, equally spaced along center lines of two equal areas of the duct cross section (station 3), were used in combustion efficiency calculations. The location of station 3 relative to the fuel atomizer tip is approximately equivalent to the turbine position in a conventional turbojet engine. By means of a suitable switching arrangement, either individual temperatures or an average temperature of all thermocouples (excluding the thermocouple located at the duct center line) could be obtained. The thermocouples were connected to a self-balancing potentiometer.

Combustor-inlet static pressure and combustor static-pressure drop were measured with absolute and U-tube manometers, respectively; the manometers were connected to static-pressure taps located at stations 2 and 4.

Combustor Fabrication

The cylindrical portion of the combustor was fabricated from 1/32-inch-thick perforated sheet steel having 1/16-inch-diameter holes on equilateral triangular centers 3/16 inch apart. Larger holes were made as required. Holes not required for a particular configuration were closed by means of metal clamp-on bands or, in the case of holes 1/8 inch in diameter or smaller, by applying a porcelain-type cement. It was possible to remove the clamp-on bands or the porcelain cement in order to reuse particular holes in later configurations.

Combustor Modifications

Air-entry-hole arrangement. - The 55 combustor configurations reported herein had four types of hole arrangement. The different types were intended to induce different air-flow patterns within the combustor, namely: rotational, funneled, zigzag, and segmented flow. Sketches showing configurations representative of each type are presented in figure 3.

Air-entry holes. - Variations in air-hole distribution, hole size, and total hole area were investigated with each type air-flow pattern. The number of air-hole variations investigated for each type flow pattern are as follows: rotational, 8; funneled, 36; zigzag, 3; and segmented, 8. The over-all range in air-hole distribution investigated is indicated by the shaded area of figure 4. Hole sizes (excluding the rectangular dilution-air slots) varied from 1/16- to 15/16-inch in diameter. Air-hole total area varied from 19.9 to 43.9 square inches.

Fuel atomizer location and combustor length. - A hollow cone, simplex-type fuel atomizer having an 80° spray angle and rated at 15.3 gallons per hour (at a pressure of 100 lb/sq in.) was used in this investigation. The distance from the face of the combustor end plate to the plane of the fuel-atomizer tip (atomizer protrusion distance) of various configurations ranged from 0 (flush) to 4.4 inches. Twenty-inch-long combustors were used with atomizer protrusion distances from 0 to 1.5 inches. Longer combustors were used with atomizer protrusion distances greater than 1.5 inches in order to maintain a distance of approximately 27 inches from the fuel atomizer to the combustor-outlet temperature-measuring plane (station 3, fig. 1).

The ignition spark gap was located at a point 1.50 inches from the combustor center line and 2.25 inches from the combustor end plate. Since the distance from the spark gap to the combustor end plate was constant for all configurations, the position of the spark gap relative to the normal fuel-spray cone varied with atomizer protrusion distance. The spark gap was located downstream of the normal spray cone for atomizer protrusion distances less than 0.5 inch and upstream for atomizer protrusion distances greater than 0.5 inch.

Ignition System

A commercial ignition plug having a 0.070-inch spark gap was used with all configurations. The ignition current was supplied by a 115-by-5000 volt, 60-cycle-per-second transformer; the estimated spark energy was 0.025 joule per spark.

Procedure

Combustor performance data were recorded for a range of fuel-air ratios at the following conditions:

Condi- tion	Combustor- inlet static pressure, in. Hg abs	Combustor- inlet tem- perature, °F	Air-flow rate ^(a) per unit area, lb/(sec)(sq ft)	Simulated flight alti- tude in reference engine at cruise speed, ft
A	15	268	2.14	56,000
B	15	268	2.78	56,000
C	8	268	1.485	70,000
D	5	268	.926	80,000

^aBased on reference cross-sectional area of 0.373 sq ft.

These conditions simulated operation of the combustor in a reference turbojet engine having a pressure ratio of 5.2 and operating at 85 percent of rated engine rotor speed at a flight Mach number of 0.6. Air-flow rates at conditions B, C, and D are representative of those used in current tubular-combustor design practice; the air-flow rate at condition A is 77 percent of current values.

Combustor reference velocity (V_r) was computed from the air mass-flow rate, the combustor-inlet density, and the reference cross-sectional area. The reference cross-sectional area (0.373 sq ft) was that of an imaginary combustor housing having an area 1.75 times the cross-sectional area of the combustor liner.

Combustion efficiency is defined as the ratio of actual enthalpy rise across the combustor (between stations 1 and 3, fig. 1) to the enthalpy supplied by the fuel and was computed by the method of reference 2. Inspection data for the MIL-F-5624A grade JP-4 fuel used in this investigation are shown in table I. The static-pressure loss between the combustor housing and the outlet duct (stations 2 and 4, fig. 1) is presented in terms of the dimensionless parameter $\Delta P/q_r$. The reference dynamic pressure q_r was computed from the inlet-air density and the combustor reference velocity V_r .

Since each combustor configuration was modified in order to produce succeeding configurations, the reproducibility of data during the investigation was not determined. From previous experience with similar apparatus, it is estimated that the values of combustion efficiency reported herein are reproducible within ± 3 percent.

RESULTS AND DISCUSSION

Combustion-efficiency data obtained with 55 different combustor configurations are presented in figures 5 to 8. Internal air-flow pattern, air-entry-hole distribution, total air-hole area, and air-hole size were varied. The data are grouped in figures 5 to 8 according to type of internal air-flow pattern and operating condition. For simplicity, individual configurations are not treated in these figures; rather, the figures indicate the over-all difference in performance obtained with a large variety of turbojet combustor designs. A brief description of the design and performance of several individual configurations is presented in table II.

Curves are faired through data points (figs. 5 to 8) that represent the maximum and minimum combustion efficiencies obtained throughout the fuel-air-ratio range. It is noted that, in general, at the high-pressure conditions (A and B), the difference in combustion efficiency of the

2934

various configurations was small over most of the fuel-air-ratio range investigated and that the greater differences occurred at the lower fuel-air ratios. At the low-pressure conditions (C and D), the greater differences sometimes occurred at high fuel-air ratios, indicating more critical rich-mixture conditions at the lower pressures. In addition, detailed inspection of the data indicated that no one configuration had the highest combustion efficiency at all conditions investigated.

Best Performing Configurations

From the 55 configurations, three were chosen to represent the best performance obtainable, each with respect to one of the following characteristics: (1) combustion efficiency at a pressure of 8 inches of mercury (condition C), (2) combustion efficiency at a pressure of 5 inches of mercury (condition D), and (3) minimum ignition-pressure limit. Design details of the three selected configurations are presented in figure 9; the operational data, in table III; and the combustion efficiency data, in figure 10. Configurations 75 and 79 had the highest combustion efficiency over a wide fuel-air-ratio range at conditions C and D, respectively; configuration 87 had the lowest ignition-pressure limit.

For a comparison of performance trends, combustion-efficiency data obtained with a current production-model turbojet combustor (ref. 3) are included in figure 10. The absolute performance level of the experimental combustors should not be compared with that of the production-model combustor. The production-model combustor was of smaller diameter, and the basis for its design included factors beyond the scope of the present investigation, such as carbon deposition, wide operating ranges, and durability problems encountered at low altitude.

At conditions A and B, the combustion efficiency of the experimental combustors (fig. 10) was essentially constant over the fuel-air-ratio range investigated; at the low-pressure conditions C and D, however, combustion efficiency decreased with an increase in fuel-air ratio. The observed effect of fuel-air ratio indicates that the experimental combustors had a rich primary-zone mixture condition at low operating pressures. In contrast, the combustion efficiency of the production-model combustor increased with an increase in fuel-air ratio at operating conditions A, B, and C, indicating a lean primary-zone mixture condition at low fuel-air ratios. This lean-mixture condition may account for the fact that burning was not possible at condition D with the production-model combustor (ref. 3).

A correlation of the combustion efficiency data of the three selected configurations with a combustion parameter V_r/P_1T_1 (reciprocal of the parameter used in ref. 4) is presented in figure 11 (V_r is the combustor

reference velocity; P_i , the combustor-inlet absolute static pressure; and T_i , the combustor-inlet absolute temperature). In figure 11(a) it the combustor-inlet absolute static temperature). In figure 11(a) it will be noted that, for a combustor temperature rise of 680° F, the highest combustion efficiency obtained at a pressure of 15 inches of mercury (condition B) was 94 percent; at a pressure of 8 inches of mercury (condition C), 85 percent; and at a pressure of 5 inches of mercury (condition D), 67 percent. Combustion efficiencies obtained for a temperature-rise of 1180° F (fig. 11(b)), at conditions A, B, and C, were only slightly lower than those obtained for 680° F at similar inlet conditions.

The ignition-pressure limit of configuration 87 was lower than its stable-burning pressure limit with the ignitor off. At air-flow rates of 0.93 and 1.47 pounds per square foot (based on a reference combustor housing cross-sectional area of 0.373 sq ft), ignition was obtained at pressures of 3.8 and 5.0 inches of mercury absolute, respectively, with a spark energy of approximately 0.025 joule per spark. Reference 5 indicates that, for a production-model combustor with comparable ignition equipment, the pressure required for ignition is considerably higher than the minimum pressure at which stable burning is obtained.

Representative combustor-outlet temperature profiles at station 3 (see fig. 1) for configurations 75 and 79 are presented in figure 12. Configuration 79 (fig. 9), which had the larger dilution-air slots and no closely spaced small holes in the downstream portion of the combustor, had lower temperature gradients.

The static-pressure losses of the three selected configurations for a range of inlet-to-outlet density ratios are presented in figure 13. The data of figure 13 indicate the pressure loss occurring inside the combustor liner only. Pressure-loss data obtained in other investigations usually include, in addition, the loss due to air flow through a relatively small annular area between the liner and the combustor housing.

Inasmuch as the experimental combustors were not investigated at high-pressure conditions, little is known concerning the durability of the liner and ignition plug or the carbon forming tendencies.

Effect of Combustor Design on Performance

In the present experimental investigation, only limited data were obtained to indicate the effects of systematic variations in combustor geometry on combustor performance. An attempt was made, nevertheless, to analyze combustor performance with respect to the design parameters investigated: internal air-flow pattern, air-entry area, air-hole size, and combustor geometry upstream of the fuel-spray cone.

Effect of internal air-flow pattern. - A comparison of the maximum combustion efficiencies (the upper envelope curves from figs. 5 to 8) obtained with each of the four different air-flow patterns is presented in figure 14. It is noted that the maximum combustion efficiencies obtained with funneled-flow configurations, at any fuel-air ratio or operating condition, were approximately equal to or higher than those obtained with any of the other configurations. Also, individual funneled-flow configurations had the widest operable fuel-air-ratio ranges at conditions C and D. None of the segmented-flow configurations would burn at condition D.

It is of interest to note that the high combustion efficiencies obtained with some configurations at low fuel-air ratios (fig. 14) were not obtainable at high fuel-air ratios regardless of air-hole geometry used.

Combustor-outlet gas-temperature profiles, obtained at station 3, for representative funneled-, segmented-, and zigzag-flow configurations are presented in figure 15. These three configurations had a similar dilution-air-hole geometry at the downstream portion of the combustor. It is noted that the zigzag-flow configuration had an unsymmetrical outlet-temperature profile and that the temperature gradient of the segmented-flow configuration was greater than that of the funneled-flow configuration. Similar data for rotational-flow configurations were not obtained.

Of the four air-flow patterns investigated, the funneled-flow configuration gave the best over-all performance with respect to combustion efficiency, operable fuel-air-ratio and pressure ranges, combustor-wall temperature, and outlet-temperature profile. The zigzag-flow combustors produced unsymmetrical outlet-temperature profiles and hot-spots on the combustor liner. The segmented-flow and most of the rotational-flow combustors would not burn at the lowest pressure investigated.

Effect of air-entry area. - The range of variations in air-hole distribution investigated and the air-hole distribution of the three best performing configurations are indicated in figure 4. With a particular air-flow pattern, the effects of varying air-hole distribution and total air-entry area were shown to be very significant, particularly at low-pressure and low-fuel-air-ratio conditions (figs. 5 to 8). In the best performing configurations, approximately 25 percent of the total air-entry area was located in the first one-half of combustor length (fig. 4). This value is substantially in agreement with that of reference 6, which suggests that approximately 20 percent of the total air-entry area be located in the first one-half of combustor length. A marked reduction, below 20 percent, in percentage total air-entry area within the first one-half of combustor length resulted in a downstream shift of the visible flame front at high fuel-air ratios, indicating over-rich primary-zone mixture conditions.

Analysis of data obtained with all configurations indicated the importance, with respect to combustion efficiency and operable fuel-air ratio and pressure ranges, of air-entry area in the upstream portion of the combustor. An illustration of the trends noted is shown in figure 16. Four combustors were investigated that varied only in air-entry area within 4 inches of the fuel-atomizer tip. At condition C (fig. 16(a)), it is noted that, as the air-entry area near the fuel atomizer was increased, the combustion efficiency increased at rich fuel-air ratios and decreased at lean fuel-air ratios, indicating a reduction of primary-zone fuel-air ratios. The peak combustion efficiency at condition C, however, was not affected by variations in primary-zone air-entry area. At condition D (fig. 16(b)), an increase in air-entry area increased both the rich and lean blow-out fuel-air ratios.

The effects of variations in total air-hole area on combustion efficiency were not systematically investigated. In general, it was observed that for configurations having reduced total air-entry area, hence higher pressure loss, combustion efficiency was less sensitive to variations in fuel-air ratio.

Effect of hole size. - Within the range investigated, variation in hole size in the downstream three-fourths of combustor length had little effect on combustion efficiency; its effect on combustor-wall temperature and exhaust-gas temperature gradient was, however, significant. The use of only closely spaced, small holes (1/16-in. diam.) throughout the combustor length confined the visible flame zone to the combustor core and produced large exhaust-gas temperature gradients. With such combustors, low temperatures on the liner walls were observed. Configurations having only widely spaced, 5/8-inch-diameter holes in the second and third quarters of combustor length produced more uniform exhaust-gas temperatures, but a substantial increase in downstream combustor-wall temperature was observed.

Visual observations of internal mixing indicated that deeper air-jet penetration resulted from the use of the larger holes and that the greater circumferential spacing between the large air jets permitted the flame path to approach the combustor wall. In general, high wall temperatures were observed with any configuration in which relatively large areas of the combustor wall had no closely spaced small holes. With configurations having alternate zones of closely spaced 1/16-inch-diameter holes and of widely spaced 5/8-inch-diameter holes (configuration 79 or 87, fig. 9), the visible flame boundary was observed to recede from the combustor wall at zones of small holes and to approach the wall at zones of large holes.

Another example of the effect of hole size on exhaust-gas temperature profile is shown in figure 12 (configurations 75 and 79). Configuration 79, which had larger dilution-air slots than configuration 75 (fig. 9) and no closely spaced small holes in the downstream portion, had the lower exhaust-gas temperature gradient.

Relatively cool combustor walls and low exhaust-gas temperature gradients were obtained at the operating conditions of this investigation by the use of a distribution of large and small holes as indicated for configurations 79 and 87, figure 9.

Effect of combustor geometry upstream of fuel-spray cone. - The annular volume (fig. 3(b)) bounded by the normal fuel-spray cone, the combustor wall, and the upstream end plate constituted the ignition and flame-piloting zone. A flame located in this region was considered to aid vaporization of fuel by direct heat transfer to the spray droplets and by increased combustor-wall temperature in the fuel-impingement region.

Variations in the air-entry-hole geometry, the volume of the flame-piloting region, and the spark-gap location (relative to the normal fuel-spray cone) were investigated in an effort to improve ignition and flame-piloting characteristics of the combustor. Some configurations having a large flame-piloting-region volume (fuel-atomizer protrusion distance of approximately 4.4 in.) had an air jacket surrounding the fuel-supply line in the combustor (e.g., configuration 75, fig. 9). Air entered this jacket through openings in the upstream end plate of the combustor and was discharged radially from holes in the jacket wall and axially, in an upstream direction, from curved tubes. This jacket was intended to reduce heat transfer to the fuel within the supply line, and the air jets were intended to increase the recirculation of gases in the flame piloting region. With such configurations, the ignition and flame piloting characteristics were similar to those observed with configurations having an atomizer protrusion distance of only 1.5 inches and having no jacket with air-guide tubes. With configurations 79 and 87 (fig. 9), flame piloting occurred upstream of the normal fuel-spray cone at all fuel-air ratios of the various operating conditions investigated. The minimum ignition pressures obtained for a number of configurations increased from approximately 4 to 9 inches of mercury absolute with an increase in air-flow rate for the range of air flows investigated (0.93 to 2.78 lb/(sec)(sq ft)). In general, ignition was obtained at or below the stable-burning pressure limits for combustors having a ring of six 5/8-inch-diameter holes located approximately 3 inches downstream of the plane of the atomizer, rings of closely spaced 1/16-inch-diameter holes upstream of the 5/8-inch-diameter holes (e.g., configurations 79 and 87, fig. 9), and a spark-gap located upstream of the normal fuel-spray cone. Apparently, the air-flow currents, as produced by such an air-entry-hole geometry, delivered fuel vapors upstream to the spark-gap region, and the local gas velocities were sufficiently low for initiation and propagation of flame.

Protrusion of the fuel atomizer into the combustion zone caused some prevaporization within the atomizer assembly at low fuel flows and resulted in fuel surging and combustion instability.

SUMMARY OF RESULTS

The air-entry-hole geometry of a tubular research combustor was experimentally varied to determine combustor design principles for good low-pressure performance. The following results were obtained:

1. Of the combustor configurations investigated, those having alternate zones of closely spaced 1/16-inch-diameter air-entry holes and widely spaced 5/8-inch-diameter holes gave the best over-all performance with respect to combustion efficiency, operable fuel-air-ratio and pressure ranges, exhaust-gas temperature profile, and combustor-wall temperature.

2. At conditions simulating a 5.2-pressure-ratio turbojet engine operating at 85 percent rated rotor speed, a flight Mach number of 0.6, and a combustor temperature rise of 680° F, maximum combustion efficiencies of 94, 85, and 67 percent were obtained at simulated altitudes of 56,000, 70,000, and 80,000 feet, respectively.

3. Within an ignition and flame-piloting region located upstream of the normal fuel-spray cone, ignition was obtained at or below the stable-burning-pressure limit of the combustor. With a configuration having such an ignition and flame-piloting region, ignition was obtained at a pressure of 3.8 inches of mercury absolute and an air-flow rate of 0.93 pound per second per square foot, by means of an inductance spark having an estimated energy of 0.025 joule per spark.

Lewis Flight Propulsion Laboratory
National Advisory Committee for Aeronautics
Cleveland, Ohio, July 2, 1953

REFERENCES

1. Olson, Walter T., Childs, J. Howard, and Jonash, Edmund R.: Turbojet Combustor Efficiency at High Altitudes. NACA RM E50I07, 1950.
2. Turner, L. Richard, and Bogart, Donald: Constant-Pressure Combustion Charts Including Effects of Diluent Addition. NACA Rep. 937, 1949. (Supersedes NACA TN's 1086 and 1655.)
3. Butze, Helmut F., Jonash, Edmund R.: Turbojet Combustor Efficiency with Ceramic-Coated Liners and with Mechanical Control of Fuel Wash on Walls. NACA RM E52I25, 1952.
4. Childs, J. Howard: Preliminary Correlation of Efficiency of Aircraft Gas-Turbine Combustors for Different Operating Conditions. NACA RM E50F15, 1950.
5. Foster, Hampton H.: Ignition-Energy Requirements in a Single Tubular Combustor. NACA RM E51A24, 1951.
6. Olson, Walter T., and Schroeter, Thomas T.: Effect of Distribution of Basket-Hole Area on Simulated Altitude Performance of 25 1/2-Inch-Diameter Annular-Type Turbojet Combustor. NACA RM E8A02, 1948.

TABLE I. - FUEL ANALYSIS



Fuel properties	MIL-F-5624A grade JP-4 (NACA fuel 52-53)
A.S.T.M. distillation D86-46, °F	
Initial boiling point	136
Percent evaporated	
5	183
10	200
20	225
30	244
40	263
50	278
60	301
70	321
80	347
90	400
Final boiling point	498
Residue, percent	1.2
Loss, percent	0.7
Aromatics, percent by volume	
A.S.T.M. D-875-46T	8.5
Silica gel	10.7
Specific gravity	0.757
Viscosity, centistokes at 100° F	0.762
Reid vapor pressure, lb/sq in.	2.9
Hydrogen-carbon ratio	0.170
Net heat of combustion	18,700

TABLE II. - DESCRIPTION AND PERFORMANCE OF INDIVIDUAL CONFIGURATIONS

[As noted in the text, the major differences in performance of the various configurations occurred mostly at the low-pressure conditions, C and D.]



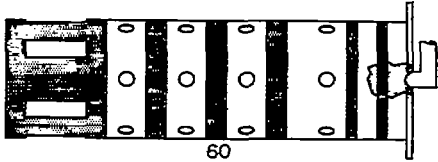
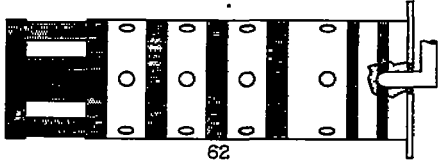
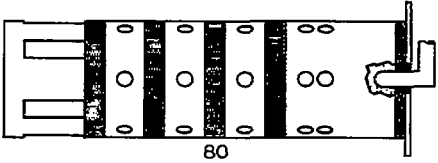
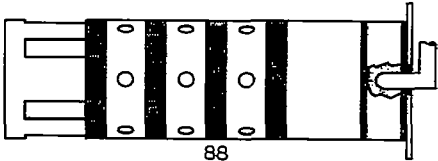
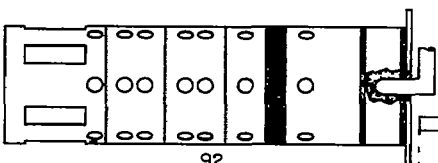
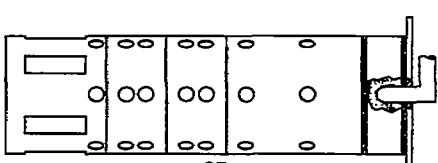
Configuration	Description	Performance
 <p style="text-align: center;">60</p>	Fuel atomizer flush with end plate. Total hole area, 40.9 sq in. Hole area within $4\frac{1}{2}$ in. of atomizer, 3.8 sq in.	Combustion efficiency at condition D varied from 82 to 65 percent in fuel-air-ratio range from 0.010 to 0.014. Rich blow-out at 0.0144.
 <p style="text-align: center;">62</p>	Fuel atomizer protrudes $\frac{1}{2}$ in. Otherwise identical with configuration 60.	Combustion efficiency at condition D varied from 87 to 54 percent in fuel-air-ratio range from 0.0125 to 0.0204.
 <p style="text-align: center;">80</p>	Similar to configuration 79 (fig. 9) except that configuration 80 has 2 rings of 5/8-in. diam. holes and fewer 1/16-in.-diam. holes in primary zone.	Combustion efficiency and operable range similar to that of configuration 79 of text. Ignition at pressure of 4.0 in. Hg abs. Good flame pilot-ing.
 <p style="text-align: center;">88</p>	Similar to configuration 87 (fig. 9) except that configuration 88 has no 5/8-in.-diam. holes in primary zone.	Combustion efficiency as much as 30 percent lower at condition C than for configuration 87. Would not burn at condition D.
 <p style="text-align: center;">92</p>	Similar to configuration 87 except that rings of 1/16-in.-diam. holes were replaced by 5/8-in.-diam. holes.	Combustion efficiency at condition D approximately 15 percent lower than for configuration 87 at comparable fuel-air ratios. High wall temperatures.
 <p style="text-align: center;">93</p>	Similar to configuration 92 except that there were no 1/16-in.-diam. holes between 1st and 2nd rings of 5/8-in.-diam. holes.	Combustion efficiency approximately 10 percent lower at condition D than for configuration 92 at comparable fuel-air ratios. High wall temperatures

TABLE II. - DESCRIPTION AND PERFORMANCE OF INDIVIDUAL CONFIGURATIONS - Continued

[As noted in the text, the major differences in performance of the various configurations occurred mostly at the low-pressure conditions, C and D.]



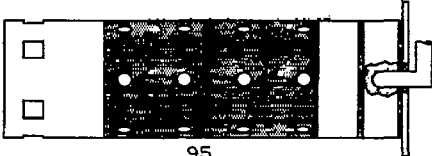
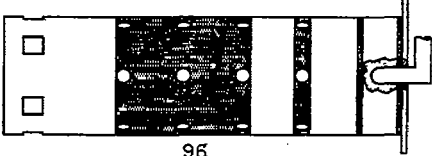
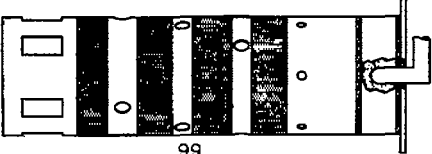
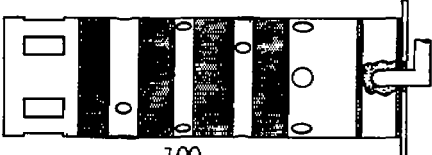
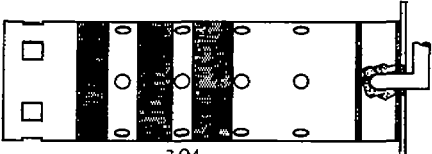
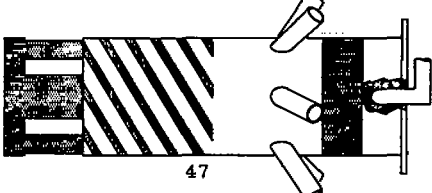
Configuration	Description	Performance
 <p style="text-align: center;">95</p>	<p>Total hole area, 34.0 sq in. Area of 1/16-in.-diam. holes, 20.6 sq in.</p>	<p>Combustion efficiency at condition D varied from 30 to 25 percent in fuel-air-ratio range from 0.014 to 0.026. Low wall temperatures.</p>
 <p style="text-align: center;">96</p>	<p>Total hole area, 32.7 sq in. Area of 1/16-in.-diam. holes, 15.6 sq in.</p>	<p>Combustion efficiency at condition D varied from 50 to 25 percent in fuel-air-ratio range from 0.016 to 0.029. Low wall temperatures.</p>
 <p style="text-align: center;">99</p>	<p>Total hole area, 31.7 sq in. Area of 1/16-in.-diam. holes, 16.0 sq in. Rings of six 7/16-in.- and of three 5/8-in.-diam. holes.</p>	<p>Combustion efficiency at condition D varied from 43 to 21 percent in fuel-air-ratio range from 0.018 to 0.026. Ignition erratic.</p>
 <p style="text-align: center;">100</p>	<p>Similar to configuration 99 except that 3/4-in.-diam. holes replace 7/16-in.-diam. holes.</p>	<p>Lean blow-out at condition D at fuel-air ratio of 0.0165. Combustion efficiency at condition D varied from 47 to 20 percent in fuel-air-ratio range from 0.017 to 0.035. Ignition at 4.9 in. Hg abs.</p>
 <p style="text-align: center;">104</p>	<p>Total hole area, 22.6 sq in. Area of 1/16-in.-diam. holes, 9.3 sq in.</p>	<p>Combustion efficiency at condition C varied from 80 to 75 percent in fuel-air-ratio range from 0.010 to 0.028; at condition D, 40 percent at 0.014. Ignition at 4.9 in. Hg abs.</p>
 <p style="text-align: center;">47</p>	<p>Total hole area, 35.0 sq in. Area of 1/16-in.-diam. holes in primary region, 3.9 sq in. Six 15/16-in. I.D. swirl generator tubes.</p>	<p>Very unsteady burning at condition C. No burning at condition D.</p>

TABLE II. - DESCRIPTION AND PERFORMANCE OF INDIVIDUAL CONFIGURATIONS - Concluded

[As noted in the text, the major differences in performance of the various configurations occurred mostly at the low-pressure conditions, C and D.]



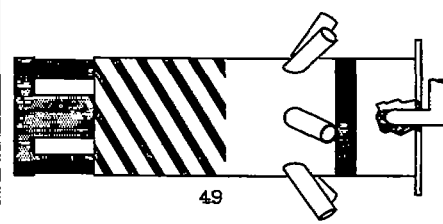
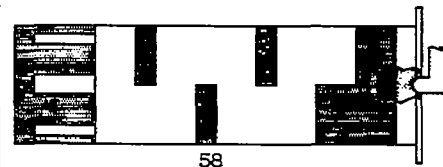
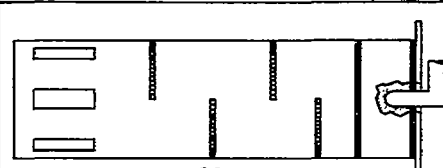
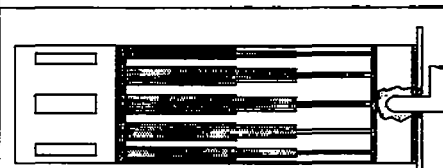
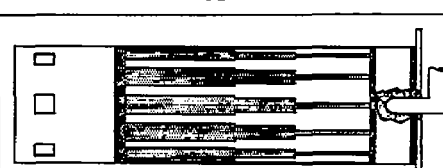
Configuration	Description	Performance
 <p>49</p>	<p>Total hole area, 32.4 sq in. Area of 1/16-in.-diam. holes in primary region, 1.3 sq in. Otherwise similar to configuration 47.</p>	<p>Combustion efficiency at condition C varied from 80 to 69 percent in fuel-air-ratio range from 0.010 to 0.018; at condition D from 61 to 48 percent in range from 0.016 to 0.026. Rich blow-out at both conditions.</p>
 <p>58</p>	<p>Total hole area, 32.6 sq in. Hole area of 1/16-in.-diam. holes in primary zone, 5.8 sq in.</p>	<p>Combustion efficiency at condition C varied from 84 to 60 percent in fuel-air-ratio range from 0.014 to 0.026; at condition D from 54 to 26 percent in range from 0.013 to 0.023. Rich blow-out.</p>
 <p>86</p>	<p>Total hole area, 30.4 sq in. Hole area of 1/16-in.-diam. holes in primary zone, 1.1 sq in. Other holes varied in diam. from 1/16 to 3/8 in.</p>	<p>Combustion efficiency at condition C similar to that for configuration 58. Would not burn at condition D.</p>
 <p>84</p>	<p>Total hole area, 40.4 sq in. Hole sizes ranged from 1/16 to 3/16-in.-diam. Dilution-air-slot area, 18.0 sq in.</p>	<p>Combustion efficiency at condition C varied from 86 to 45 percent in fuel-air-ratio range from 0.014 to 0.028. Would not burn at condition D.</p>
 <p>83</p>	<p>Total hole area, 28.4 sq in. Similar to configuration 84 except for dilution-air-slot area of 6.0 sq in.</p>	<p>Combustion efficiency at condition A varied from 41 to 89 percent in fuel-air-ratio range from 0.008 to 0.022. Would not burn at condition C or D.</p>

TABLE III. - OPERATIONAL DATA FOR THREE SELECTED COMBUSTOR CONFIGURATIONS



Run	Combustor-inlet static pressure, P_1 , in. Hg abs	Combustor inlet-temperature, T_1 , $^{\circ}R$	Air flow, lb/sec	Combustor reference velocity, V_r , ft/sec	Static-pressure drop through combustor, ΔP , in. Hg	Fuel flow, lb/hr	Fuel atomizer pressure drop, ΔP , lb/sq in.	Fuel-air ratio	Mean combustor-outlet temperature, t_{OR}	Combustion efficiency, percent
Configuration 75										
952	15.0	728	0.800	78.4	0.66	24.4	18	0.0085	1300	92.4
953	↓	↓	↓	↓	.69	29.7	16	.0103	1415	92.3
954	↓	↓	↓	↓	.77	41.8	19	.0145	1655	90.7
955	↓	↓	↓	↓	.84	51.8	34	.0180	1850	90.3
956	↓	↓	↓	↓	.89	60.3	41	.0209	1995	89.0
957	↓	↓	↓	↓	.96	66.4	47	.0231	2090	87.8
958	15.0	728	1.040	102.0	1.03	24.4	18	.0065	1185	94.9
959	↓	↓	↓	↓	1.10	34.8	16	.0093	1340	90.5
960	↓	↓	↓	↓	1.24	49.8	27	.0133	1600	92.5
961	↓	↓	↓	↓	1.34	63.0	43	.0168	1795	91.3
962	↓	↓	↓	↓	1.46	74.3	59	.0198	1945	89.8
963	8.0	728	0.560	103.0	.68	21.8	—	.0108	1490	98.1
964	↓	↓	↓	↓	.74	34.8	—	.0173	1725	85.0
965	↓	↓	↓	↓	.82	42.3	20	.0210	1900	81.8
966	↓	↓	↓	↓	.89	50.4	27	.0250	2040	78.2
Configuration 78										
1038	15.0	728	0.802	78.6	0.52	22.5	—	0.0078	1220	85.9
1039	↓	↓	↓	↓	.59	29.5	—	.0102	1405	91.7
1040	↓	↓	↓	↓	.70	41.6	17	.0144	1645	90.3
1041	↓	↓	↓	↓	.77	52.0	27	.0180	1855	89.0
1042	↓	↓	↓	↓	.83	60.7	39	.0210	1995	88.7
1043	↓	↓	↓	↓	.88	66.9	47	.0232	2100	86.1
1044	15.0	728	1.040	102.0	.86	24.7	—	.0066	1160	88.5
1045	↓	↓	↓	↓	.95	34.3	—	.0092	1360	94.9
1046	↓	↓	↓	↓	1.10	50.0	24	.0135	1600	92.2
1047	↓	↓	↓	↓	1.26	63.0	42	.0168	1780	89.9
1048	↓	↓	↓	↓	1.38	74.5	59	.0199	1945	89.5
1049	↓	↓	↓	↓	1.42	81.9	70	.0219	2045	89.0
1050	8.0	728	0.554	101.9	.51	19.7	—	.0099	1340	85.3
1051	↓	↓	↓	↓	.61	24.7	—	.0124	1470	83.7
1052	↓	↓	↓	↓	.67	34.2	—	.0172	1725	83.3
1053	↓	↓	↓	↓	.72	41.8	18	.0210	1880	80.4
1054	↓	↓	↓	↓	.77	49.8	25	.0250	1860	68.9
1055	↓	↓	↓	↓	.70	55.4	37	.0278	1765	55.3
1063	5.0	728	0.340	100.0	.37	17.4	—	.0142	1420	68.1
1064	↓	↓	↓	↓	.40	24.7	—	.0202	1620	63.6
1065	↓	↓	↓	↓	.39	28.9	—	.0236	1560	51.0
1066	↓	↓	↓	↓	.35	36.3	—	.0297	1485	37.4
1067	5.1	↓	↓	98.2	.27	42.9	—	.0350	1405	28.6
Configuration 87										
1231	15.0	728	0.805	78.7	0.54	23.3	—	0.0081	1240	86.6
1232	↓	↓	↓	↓	.60	29.8	—	.0105	1410	91.5
1233	↓	↓	↓	↓	.66	39.3	16	.0136	1590	89.5
1234	↓	↓	↓	↓	.80	53.2	30	.0184	1850	88.5
1235	↓	↓	↓	↓	.87	63.2	43	.0219	2030	88.0
1236	8.0	728	0.555	102.1	.54	20.2	—	.0101	1360	86.2
1237	↓	↓	0.557	102.5	.59	24.7	—	.0123	1470	84.1
1238	↓	↓	↓	↓	.63	28.2	—	.0141	1560	83.5
1239	↓	↓	↓	↓	.71	35.3	—	.0176	1710	80.1
1240	↓	↓	↓	↓	.75	41.7	19	.0208	1845	78.4
1241	↓	↓	↓	↓	.78	50.7	27	.0253	1830	64.3
1242	↓	↓	↓	↓	.70	54.3	31	.0271	1680	51.7
1251	5.0	728	0.350	103.0	.35	19.0	—	.0151	1300	52.9
1252	↓	↓	↓	↓	.37	23.5	—	.0186	1370	48.7
1253	↓	↓	↓	↓	.38	28.5	—	.0226	1370	40.6
1254	↓	↓	↓	↓	.37	33.0	—	.0262	1315	32.3
1255	↓	↓	↓	↓	.34	37.6	—	.0298	1200	22.9

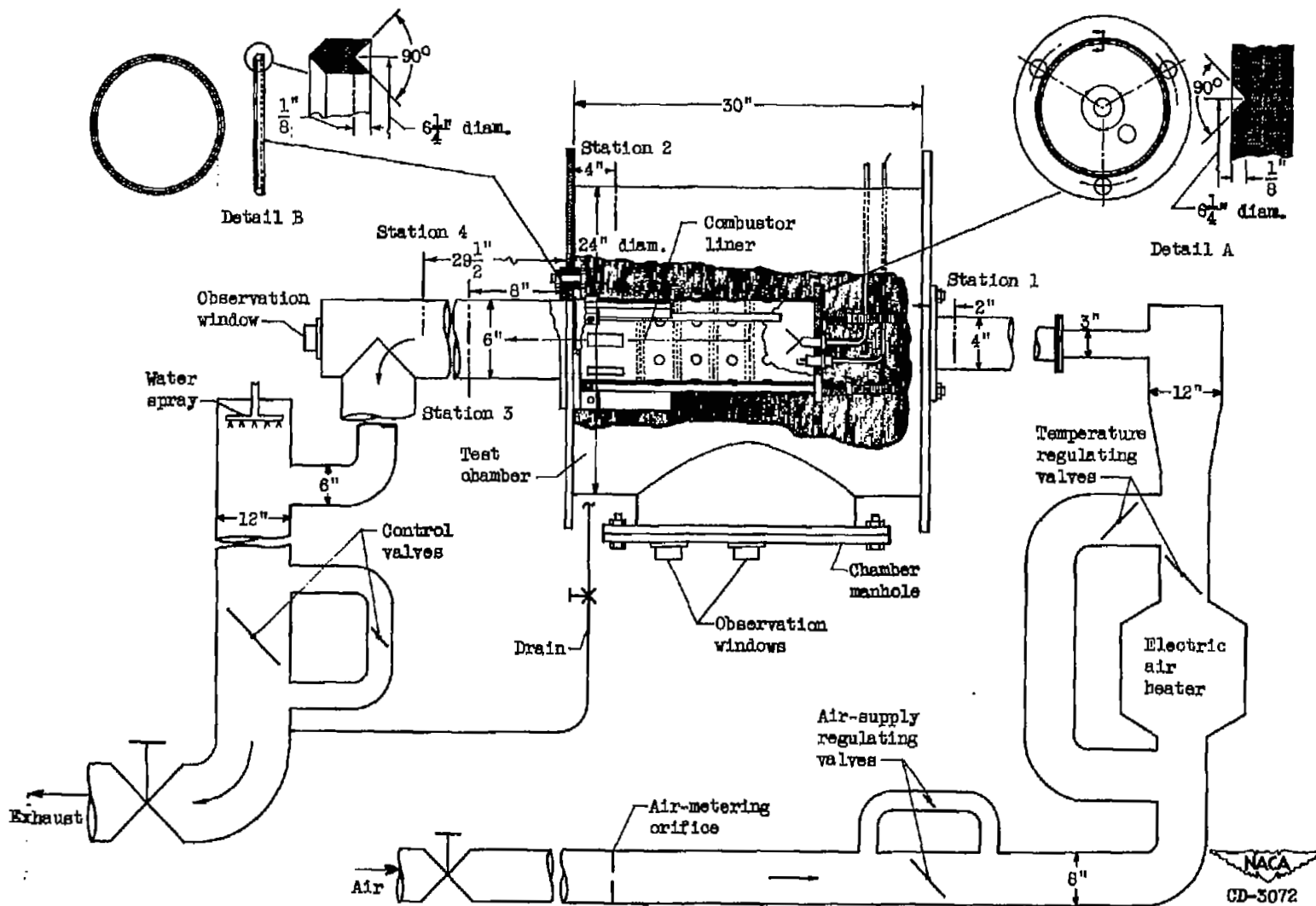


Figure 1. - Diagram of test-chamber installation showing details of chamber and combustor assembly.

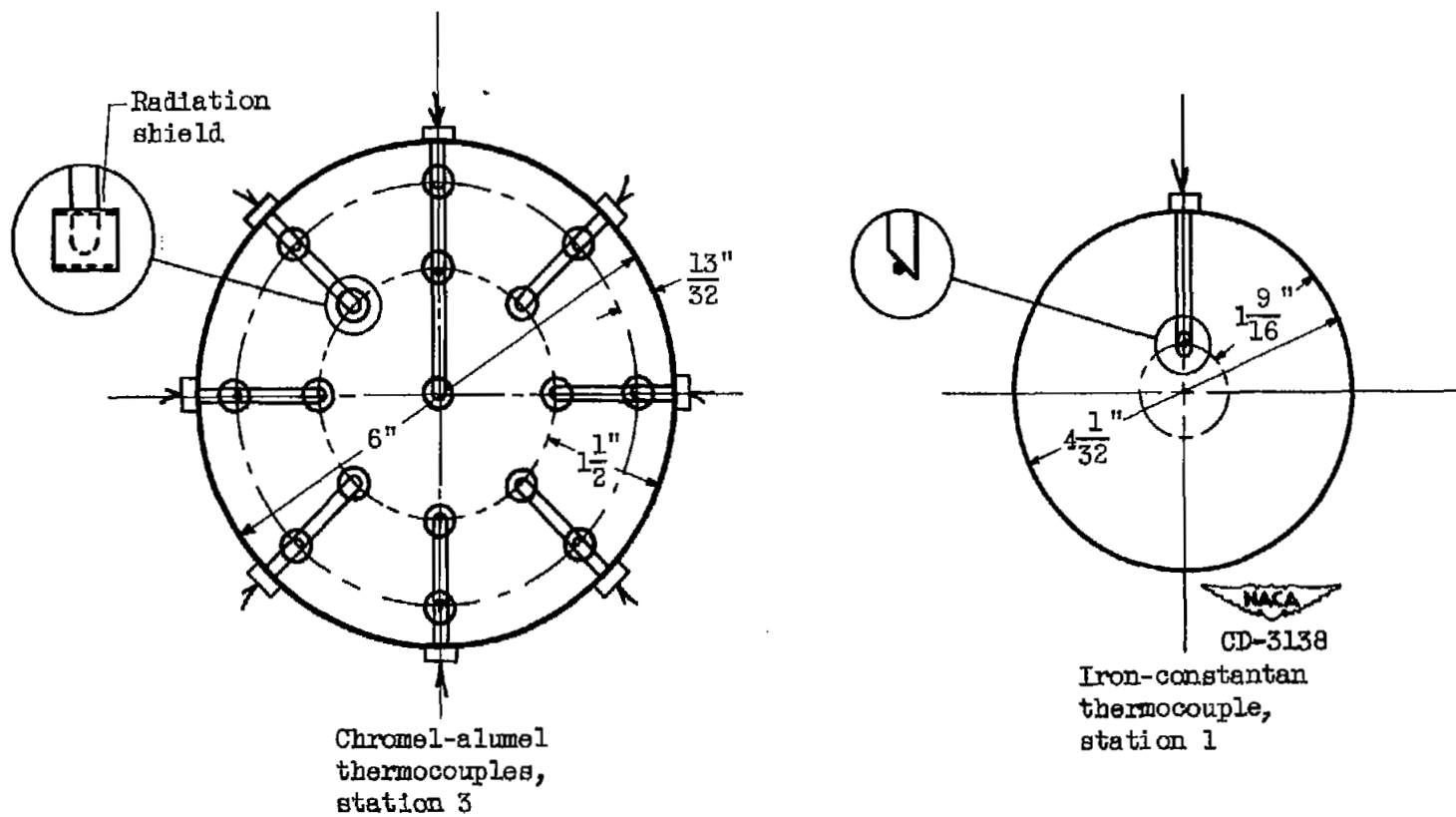


Figure 2. - Sketch showing arrangement of thermocouples at stations 1 and 3 (see fig. 1).

2934

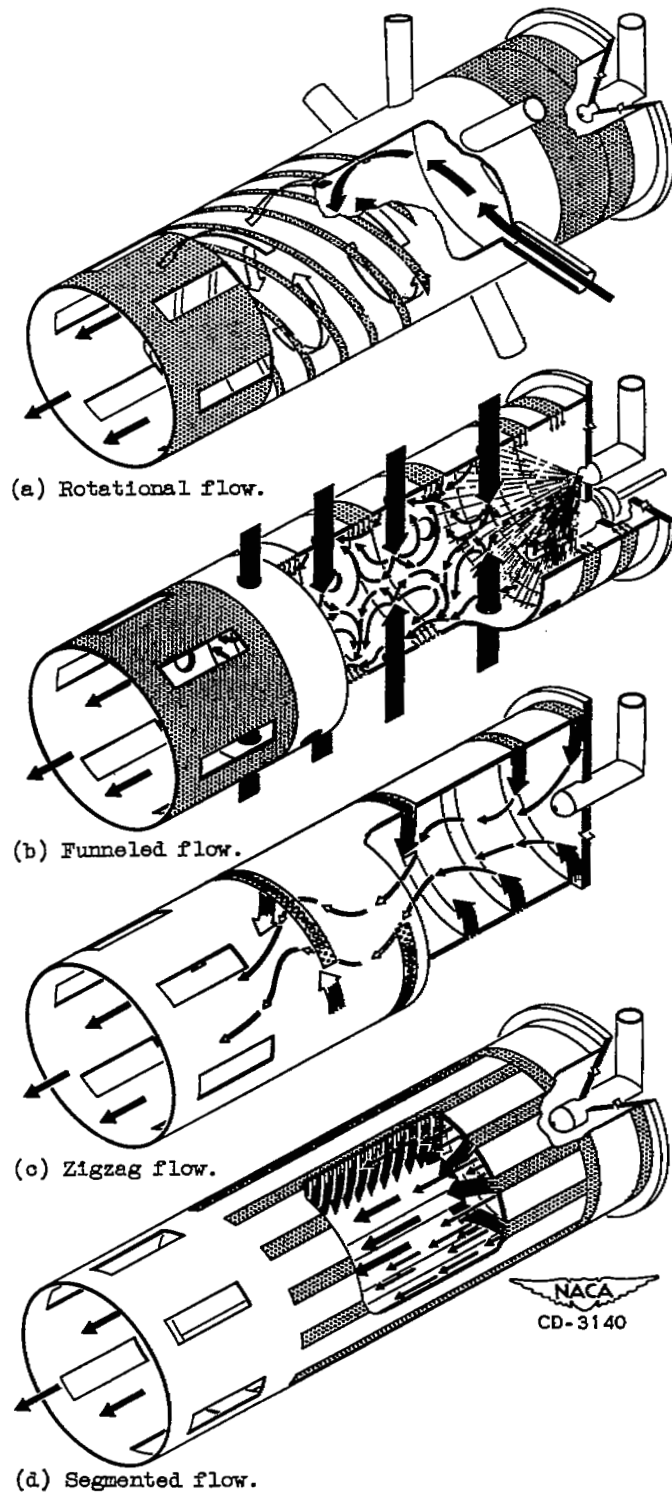


Figure 3. - Sketches of typical experimental combustor configurations showing internal air-flow patterns.

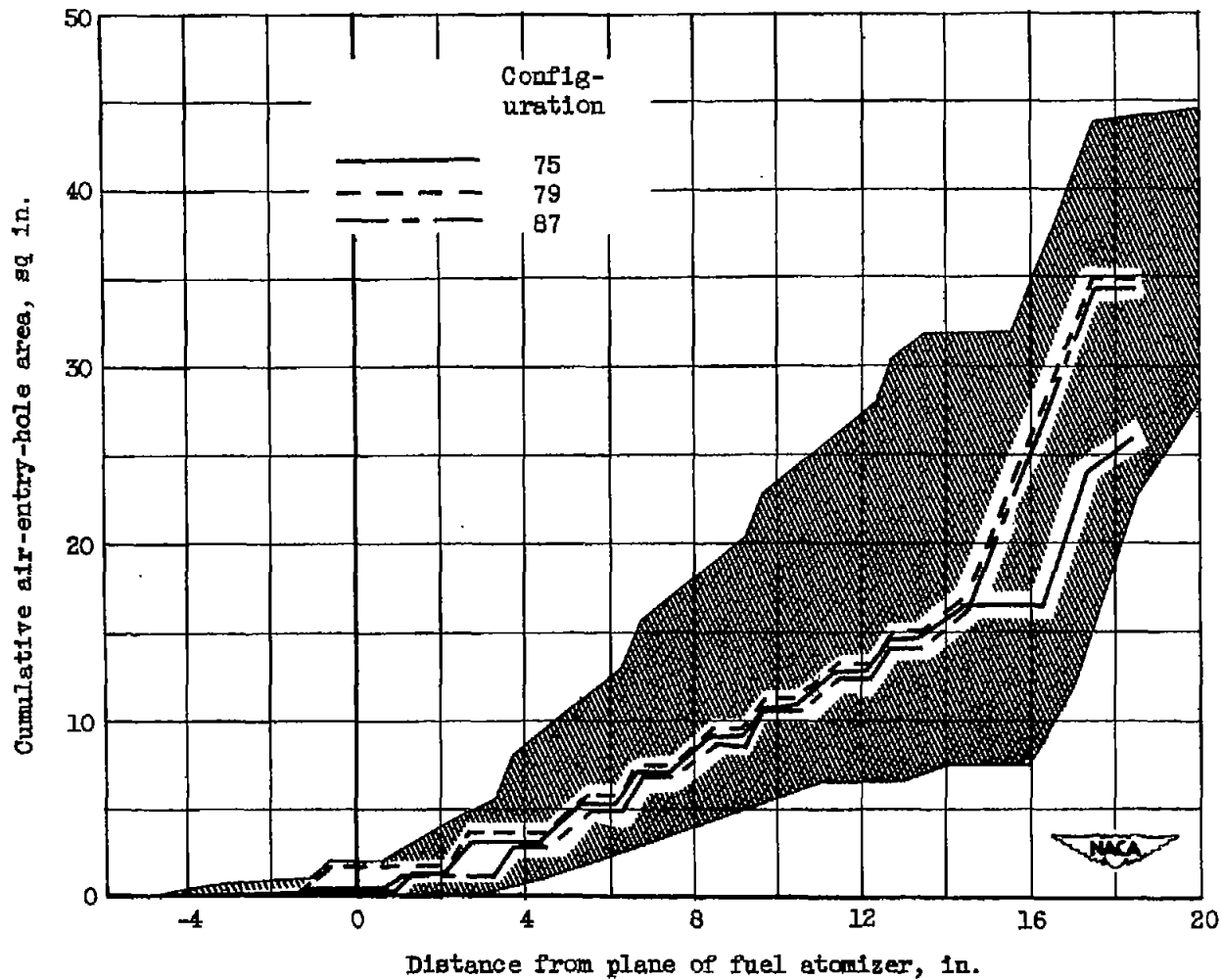
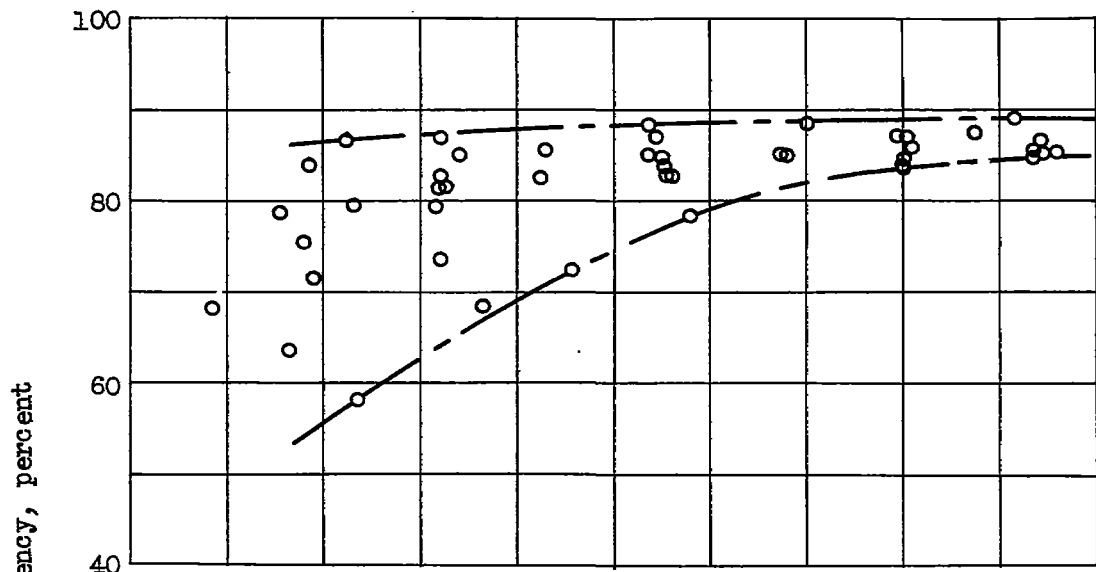
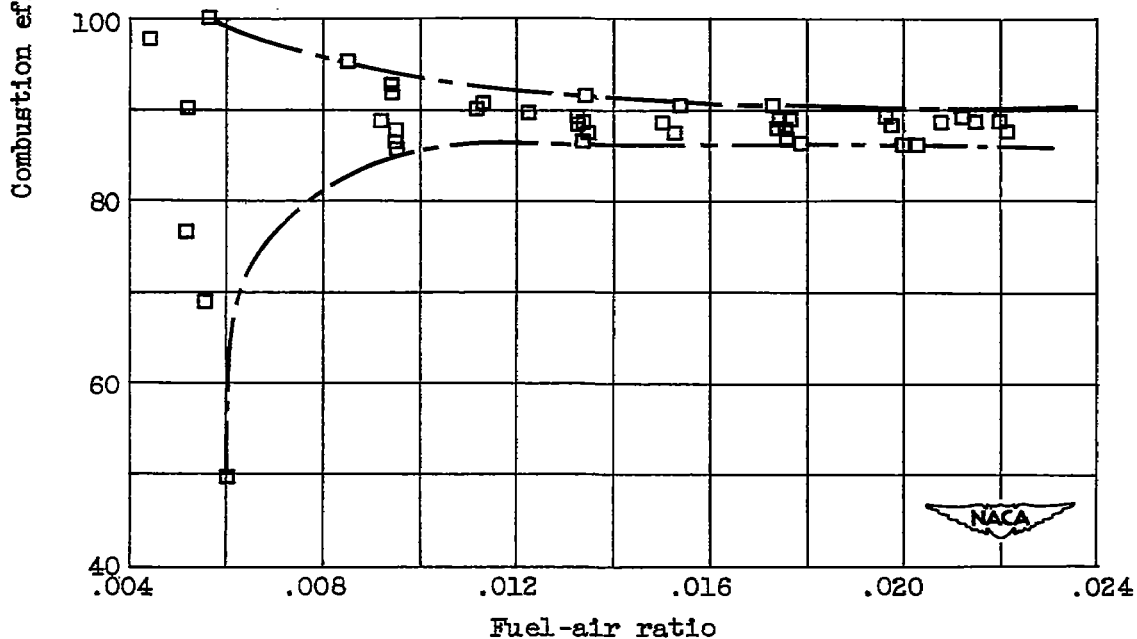


Figure 4. - Range of variation in cumulative air-entry-hole area investigated and in cumulative air-entry-hole area of three selected experimental configurations as function of distance from plane of fuel-atomizer tip.

2934

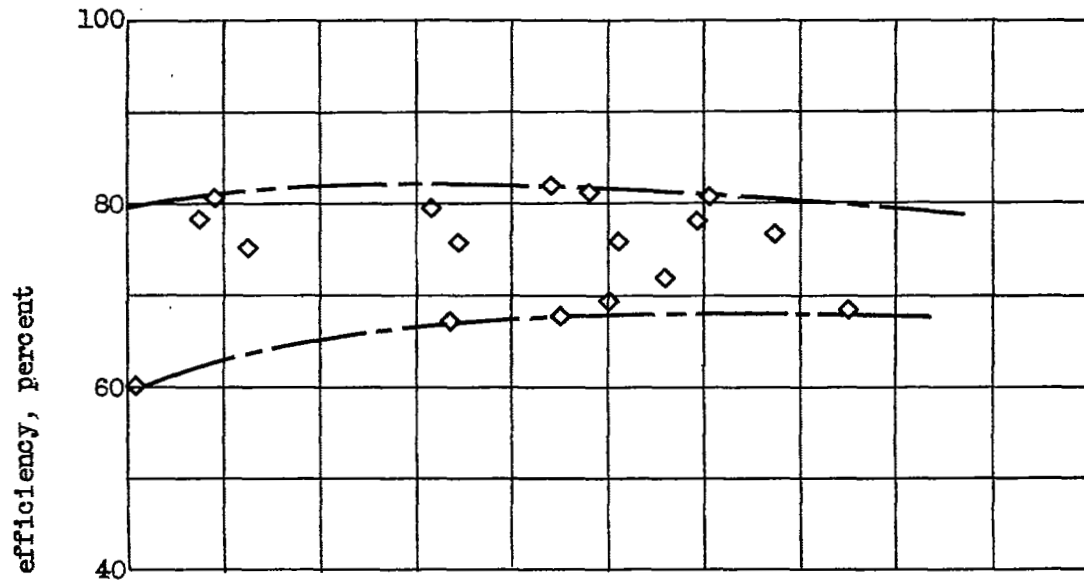


(a) Operating condition A. Data for 8 configurations.

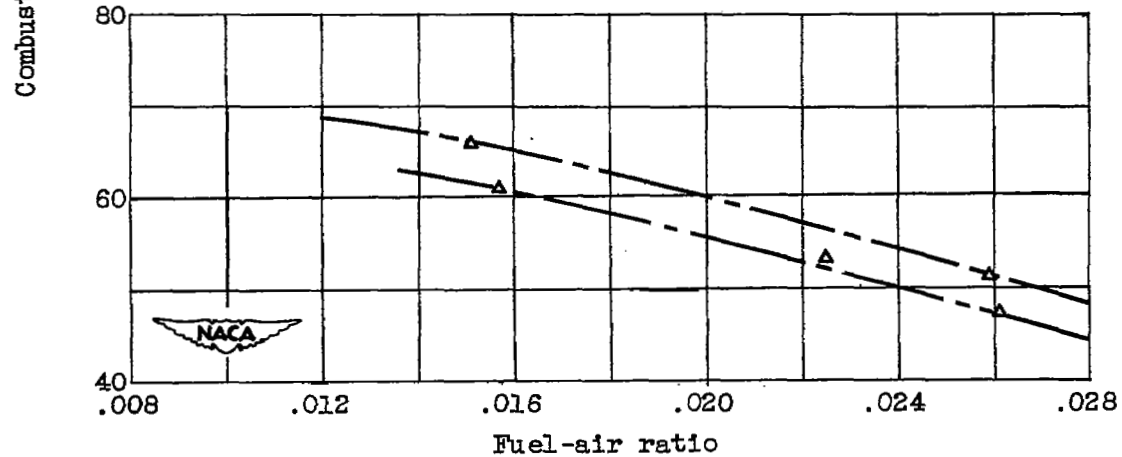


(b) Operating condition B. Data for 7 configurations.

Figure 5. - Effect of air-entry-hole geometry on combustion efficiency of rotational-flow configurations at various operating conditions.



(c) Operating condition C. Data for 6 configurations.



(d) Operating condition D. Data for 2 configurations.

Figure 5. - Concluded. Effect of air-entry-hole geometry on combustion efficiency of rotational-flow configurations at various operating conditions.

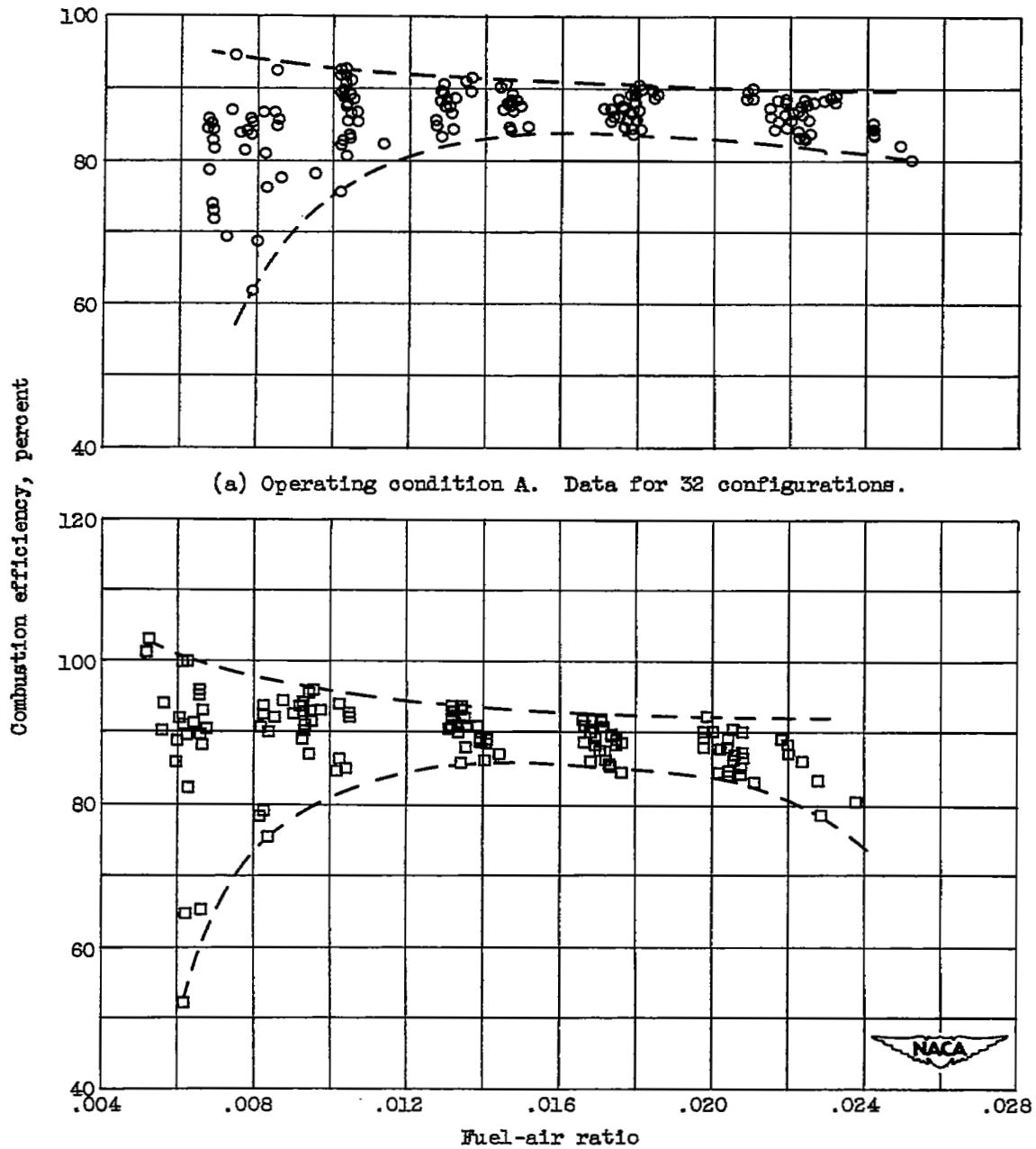
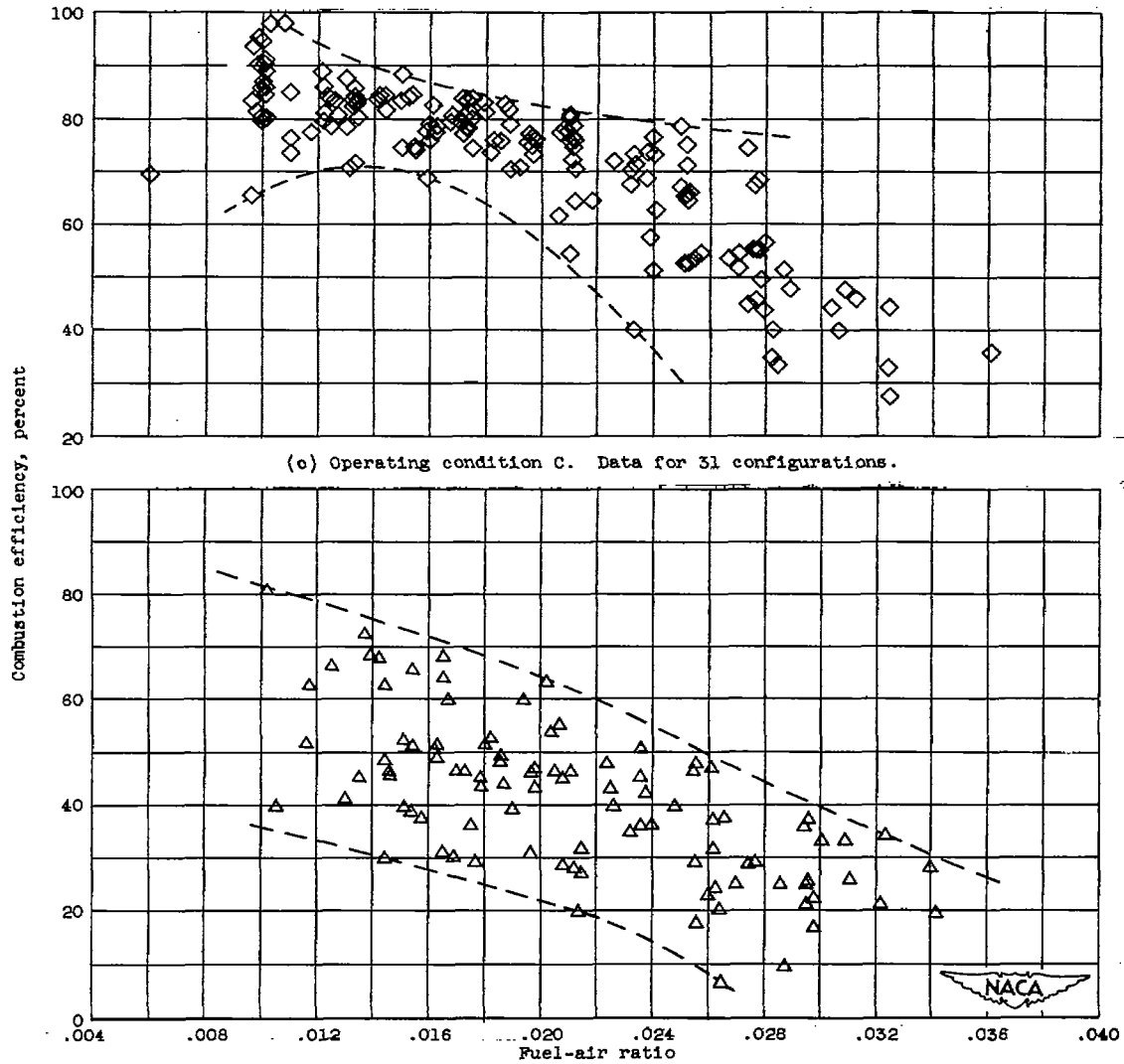


Figure 6. - Effect of air-entry-hole geometry on combustion efficiency of funneled-flow configurations at various operating conditions.



(c) Operating condition C. Data for 31 configurations.

(d) Operating condition D. Data for 29 configurations.

Figure 6. - Concluded. Effect of air-entry-hole geometry on combustion efficiency of funneled-flow configurations at various operating conditions.

2934

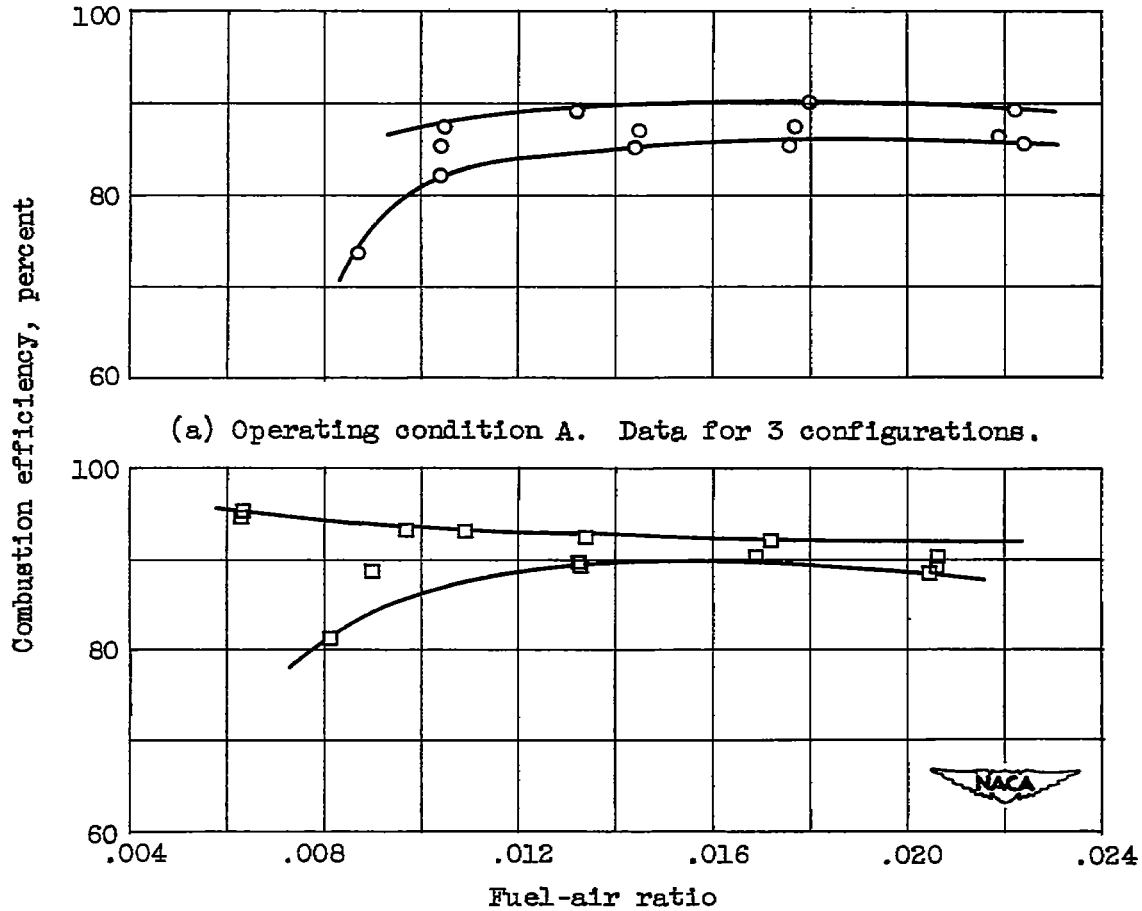


Figure 7. - Effect of air-entry-hole geometry on combustion efficiency of zigzag-flow configurations at various operating conditions.

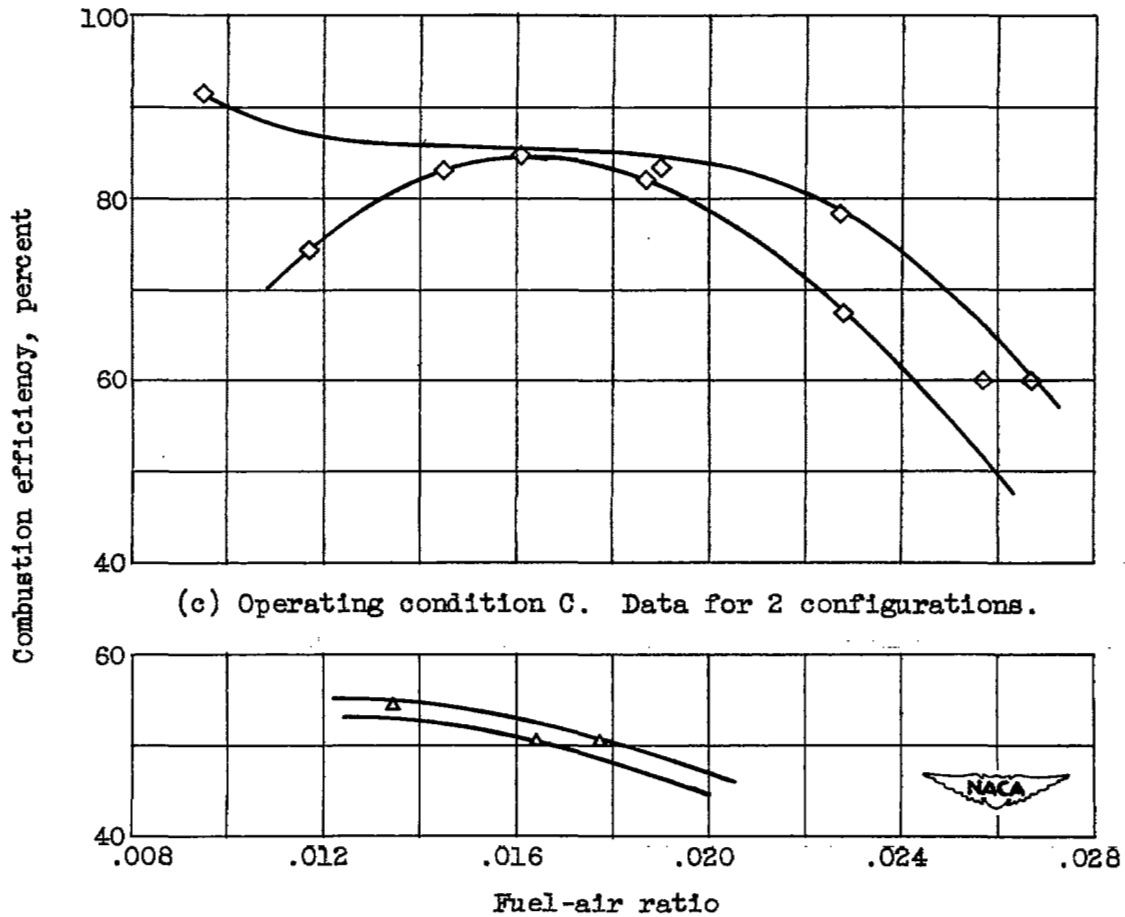
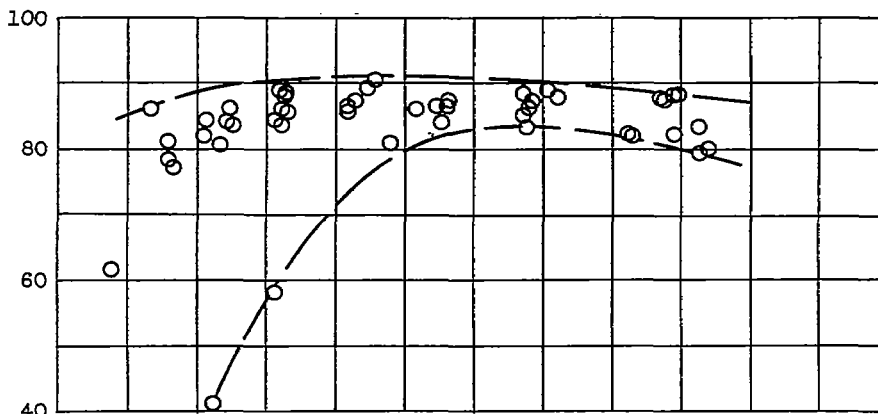
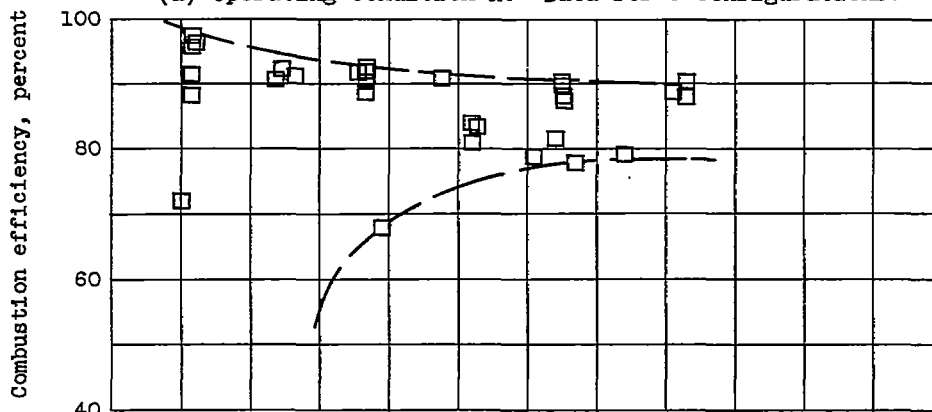


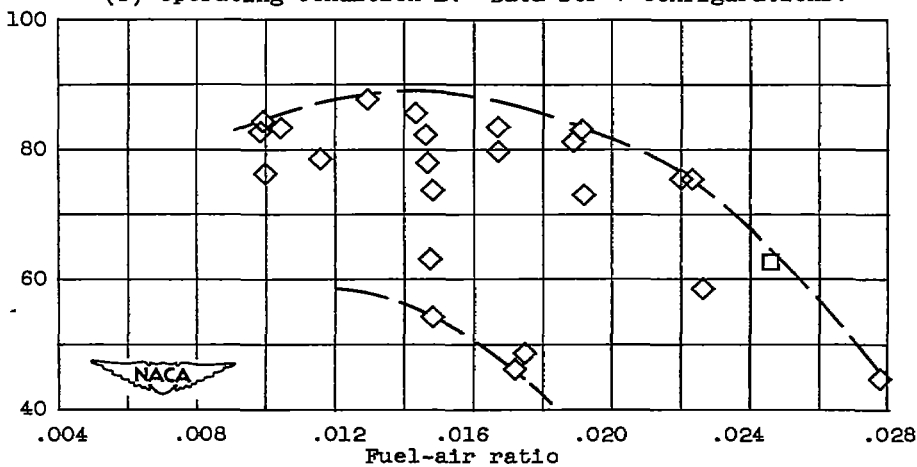
Figure 7. - Concluded. Effect of air-entry-hole geometry on combustion efficiency of zigzag-flow configurations at various operating conditions.



(a) Operating condition A. Data for 8 configurations.



(b) Operating condition B. Data for 7 configurations.



(c) Operating condition C. Data for 7 configurations.

Figure 8. - Effect of air-entry-hole geometry on combustion efficiency of segmented-flow configurations at various operating conditions.

2954 .

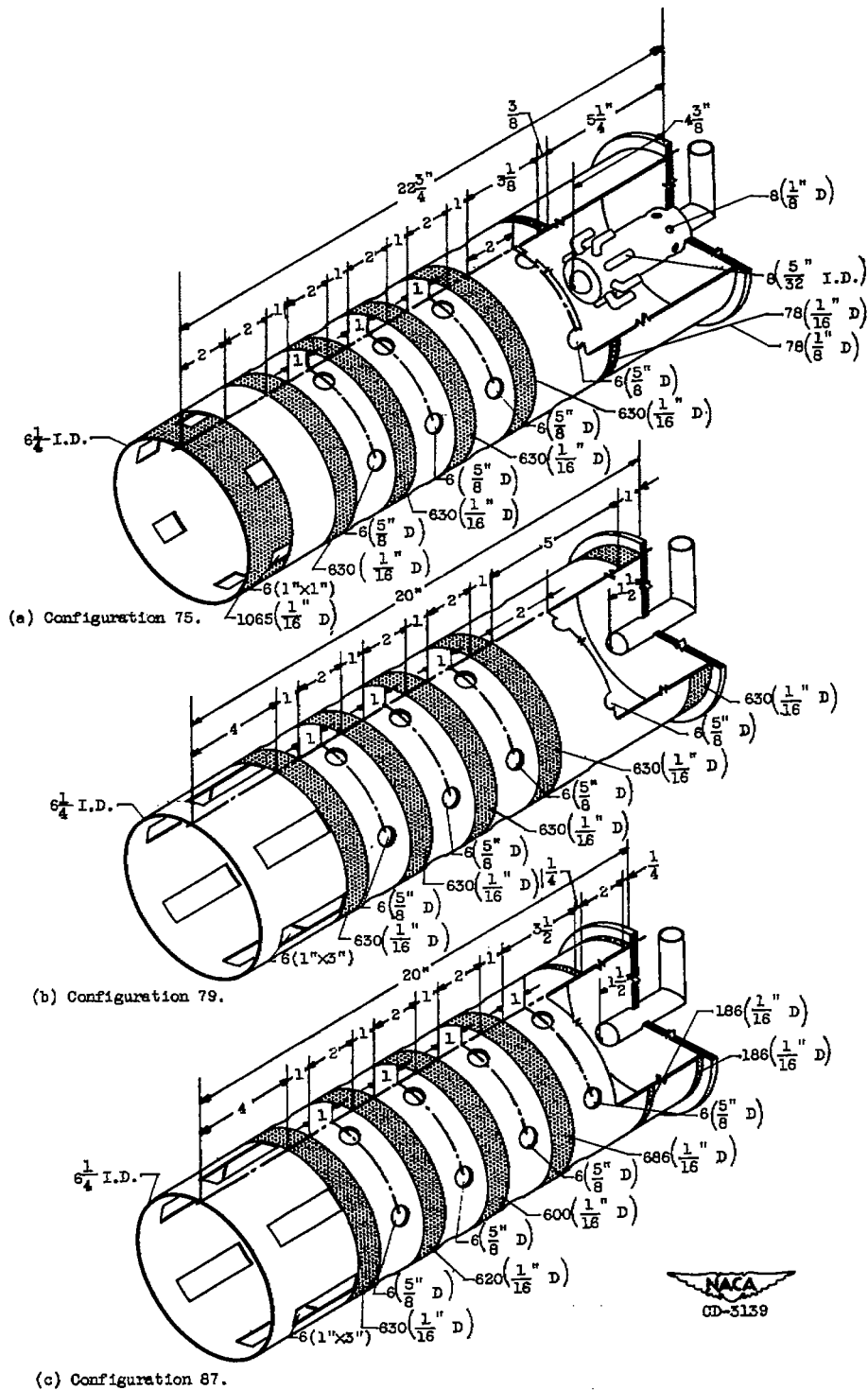
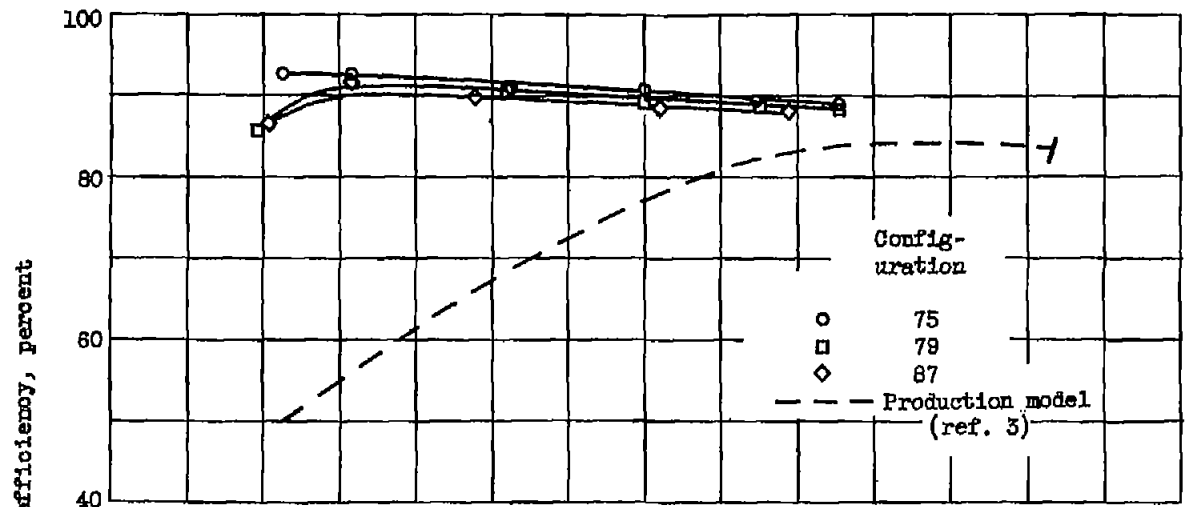
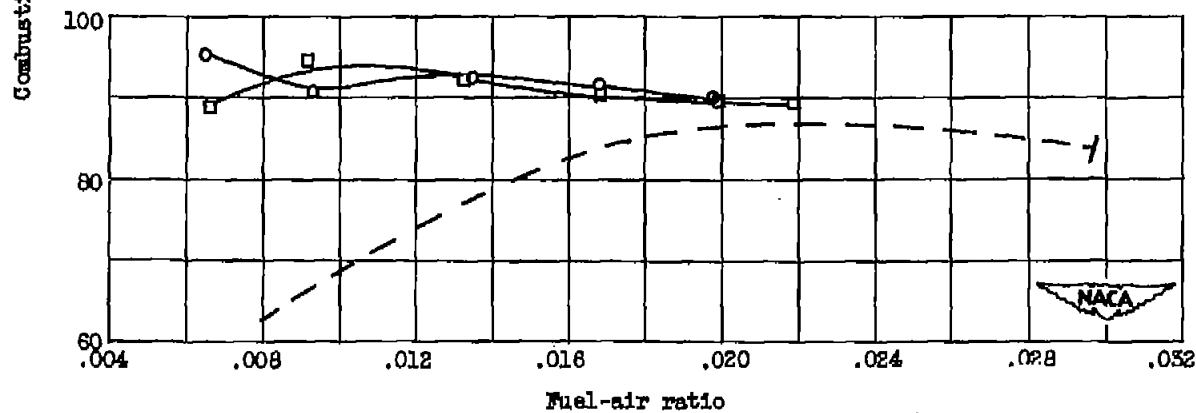


Figure 9. - Design details of three selected experimental combustor configurations showing number, size, and location of air-entry holes.

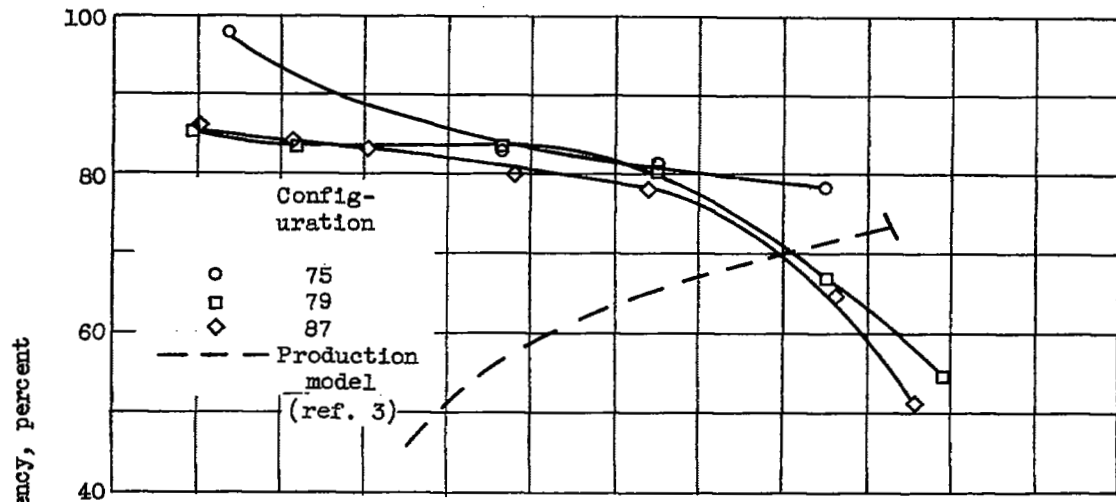


(a) Operating condition A.

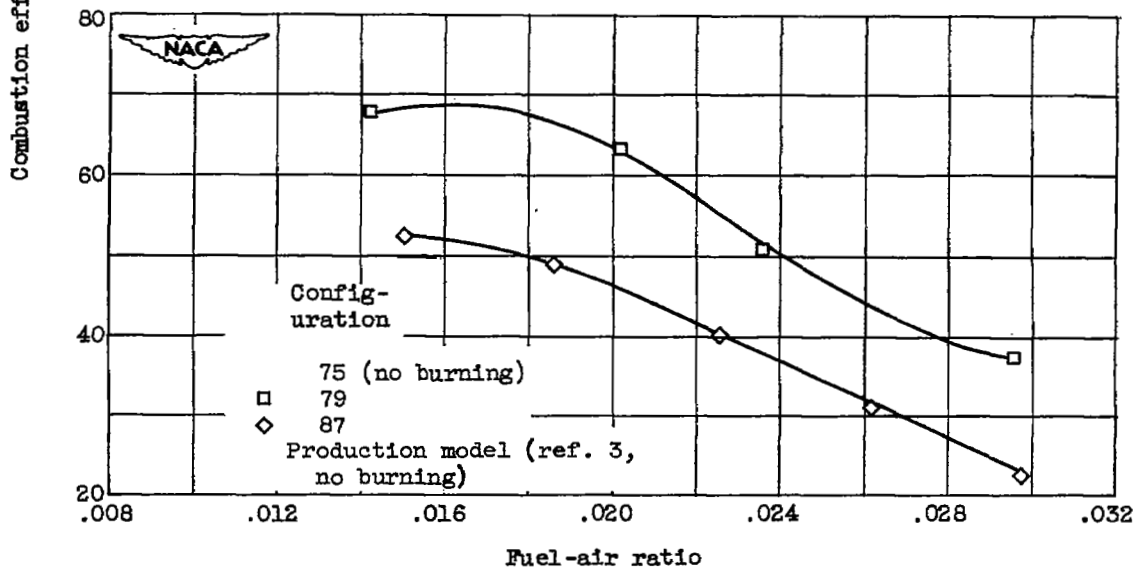


(b) Operating condition B.

Figure 10. - Combustion efficiency of three selected experimental combustors and of current production-model turbojet combustor at various operating conditions.



(c) Operating condition C.



(d) Operating condition B.

Figure 10. - Concluded. Combustion efficiency of three selected experimental combustors and of current production-model turbojet combustor at various operating conditions.

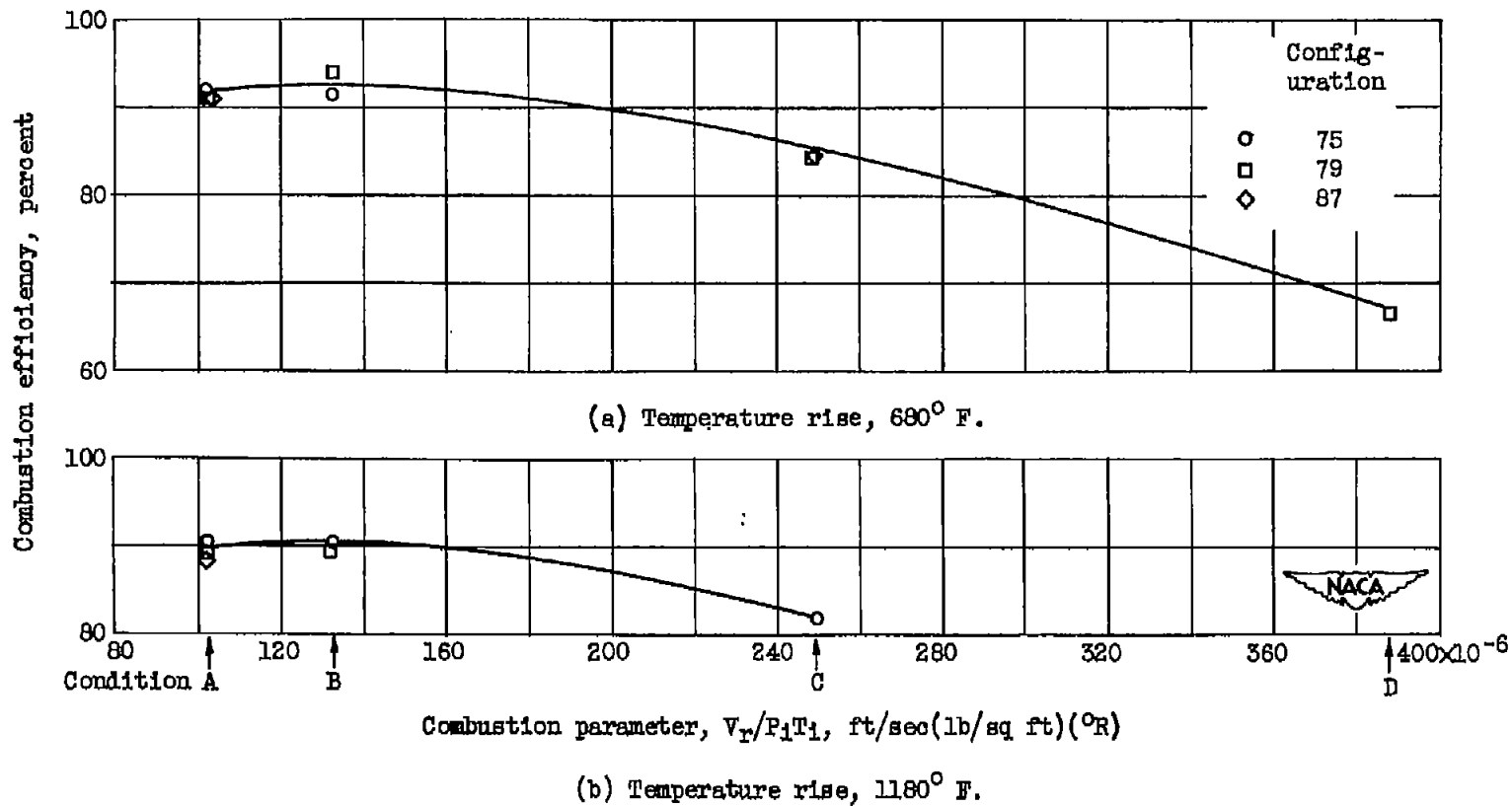
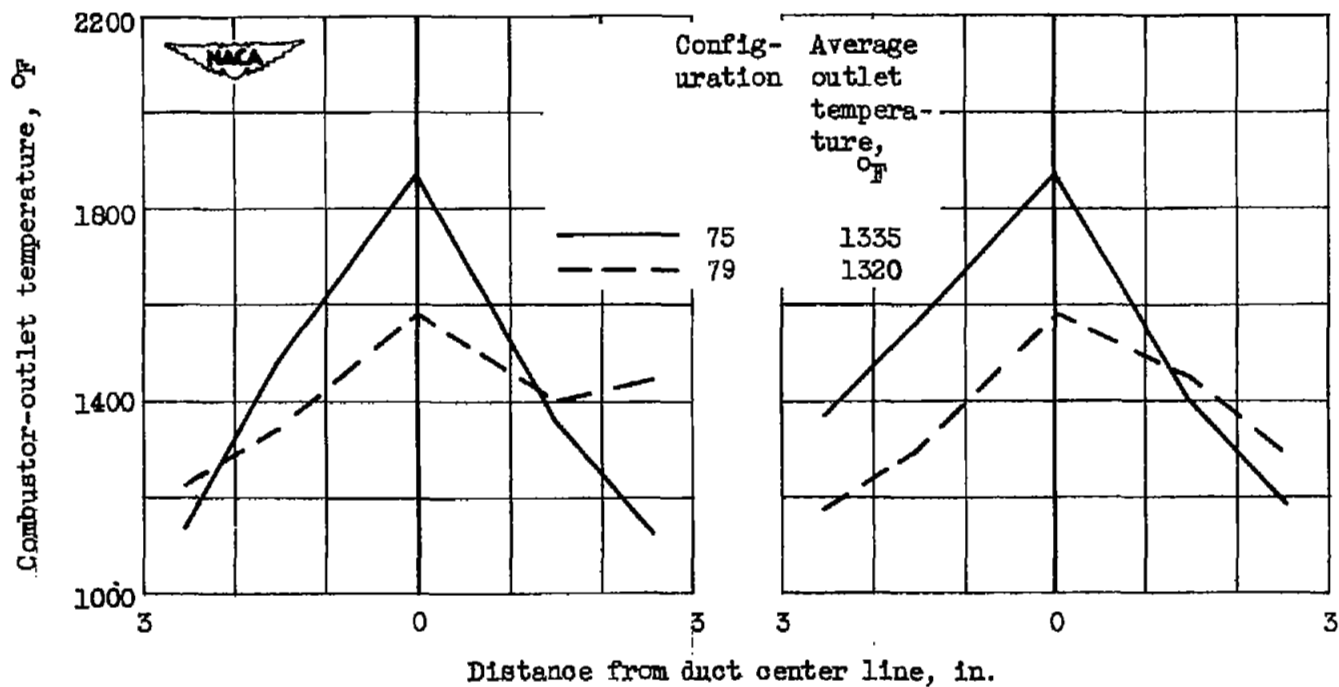


Figure 11. - Correlation of combustion-efficiency data of three selected experimental combustors with combustion parameter (ref. 4) at two values of combustor temperature rise.

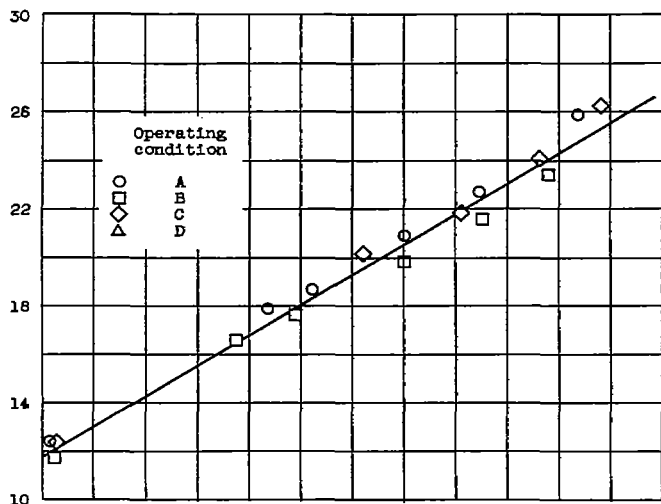


(a) Vertical traverse.

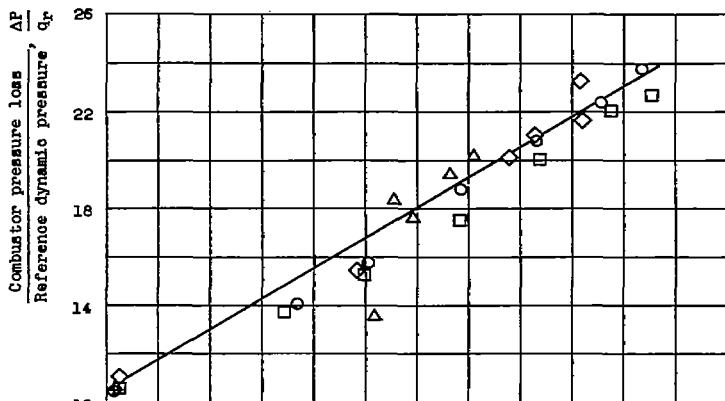
(b) Horizontal traverse.

Figure 12. - Combustor-outlet temperature profiles at station 3 and condition B for configurations 75 and 79. (Average outlet temperatures are based on average of 16 thermocouples not on center line of duct.)

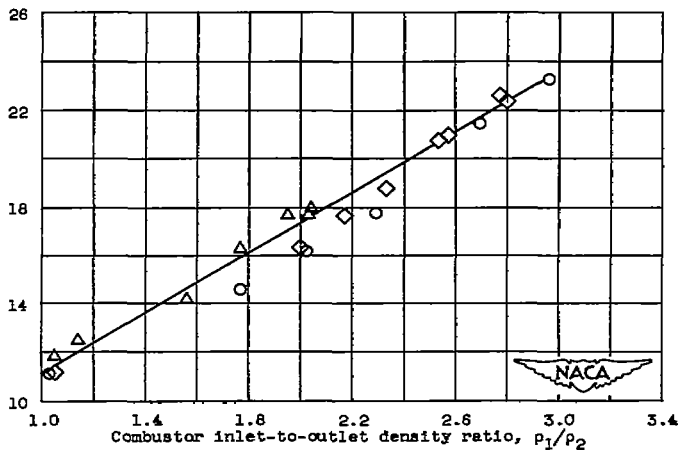
CF-5 back 2934



(a) Configuration 75.



(b) Configuration 79.



(c) Configuration 87.

Figure 13. - Static-pressure losses of three selected experimental configurations.

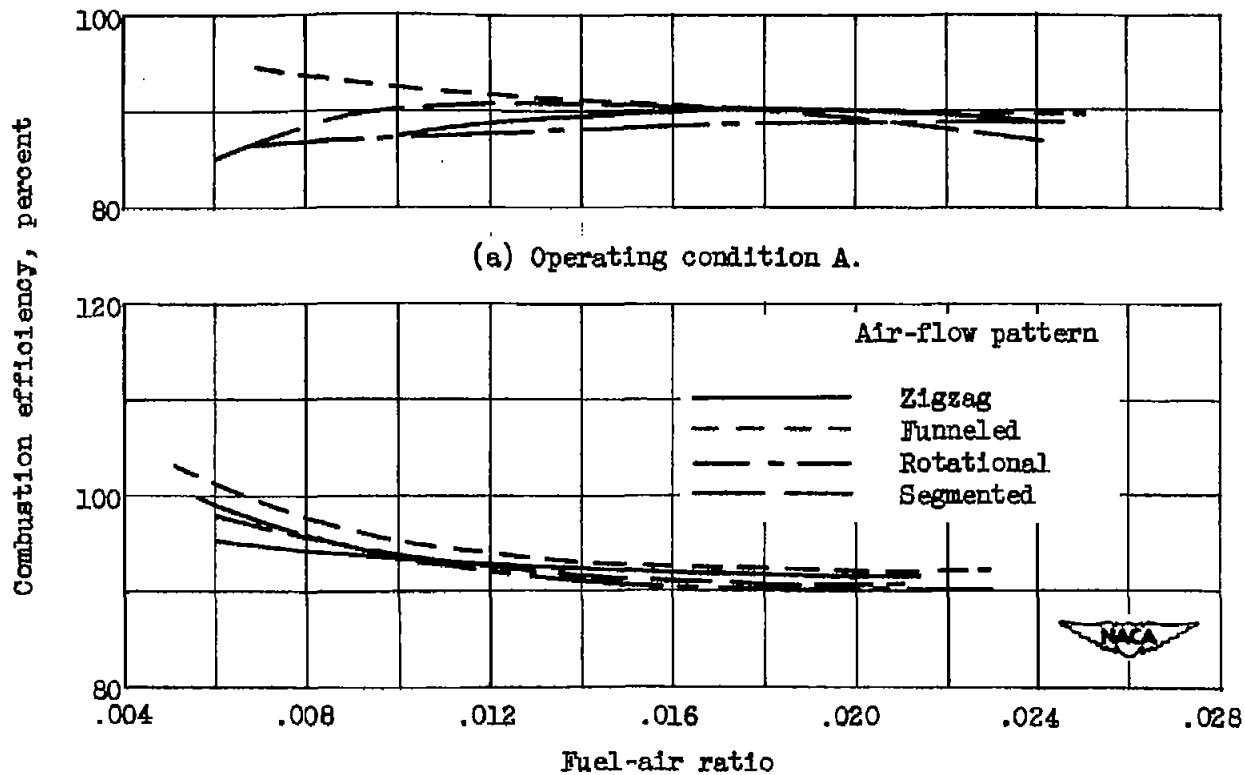
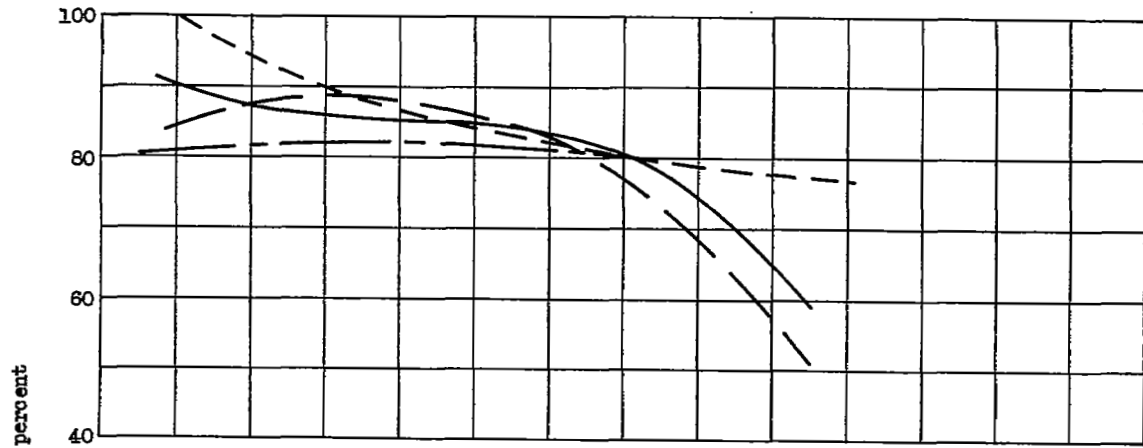
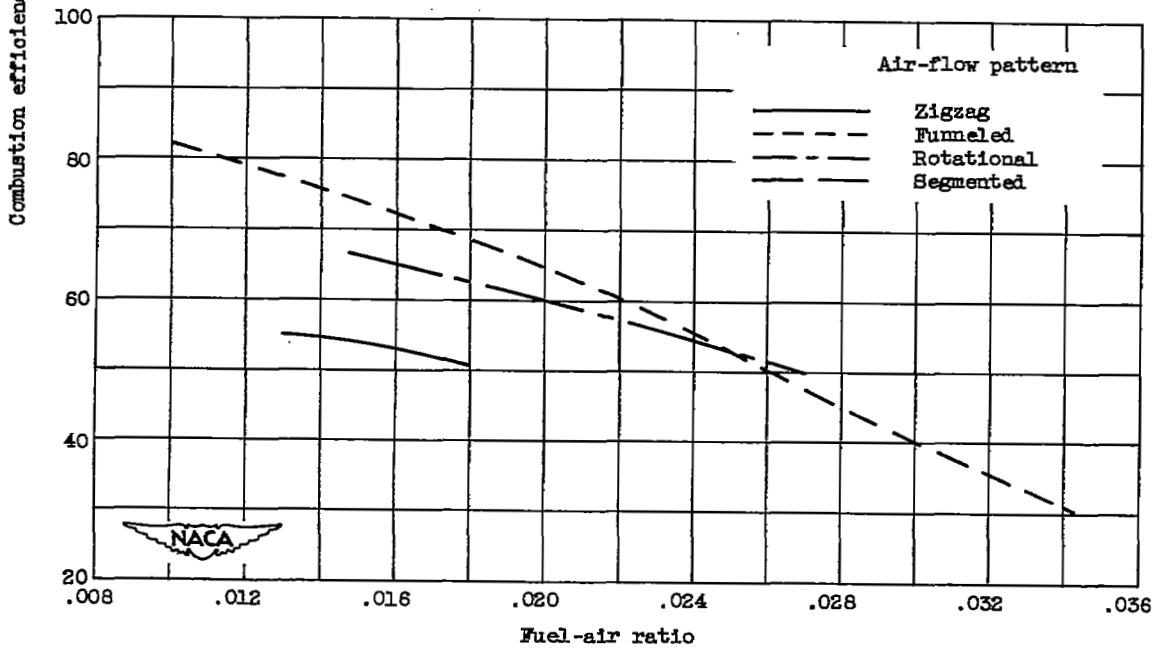


Figure 14. - Comparison of curves of maximum combustion efficiency (from figs. 5 to 8) obtained with various types of internal air-flow pattern at various operating conditions.

2934



(c) Operating condition C.



(d) Operating condition D.

Figure 14. - Concluded. Comparison of curves of maximum combustion efficiency (from figs. 5 to 8) obtained with various types of internal air-flow pattern at various operating conditions.

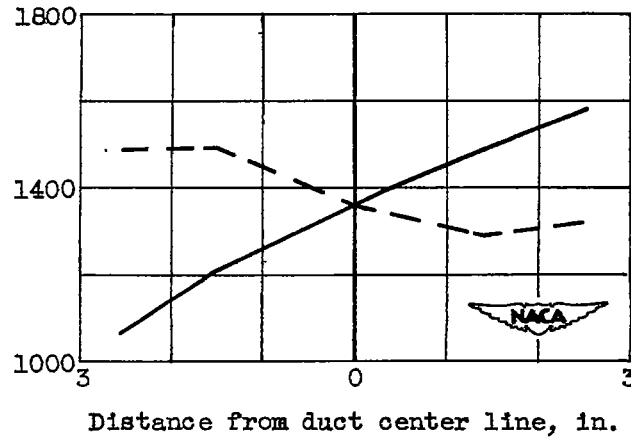
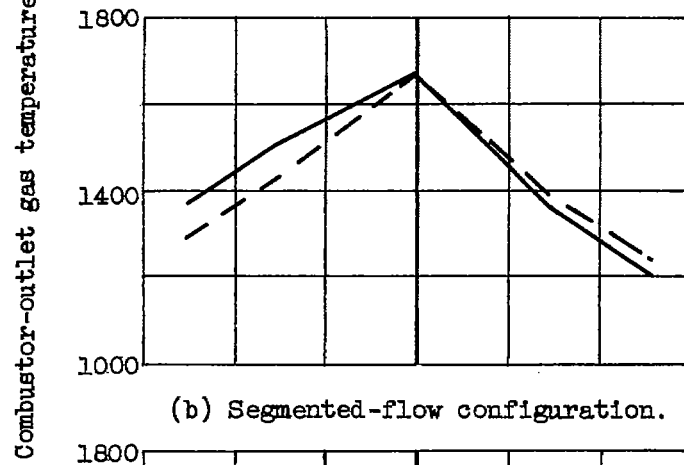
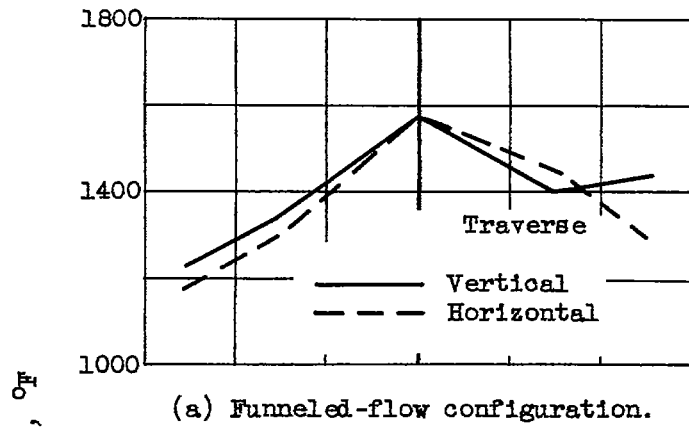
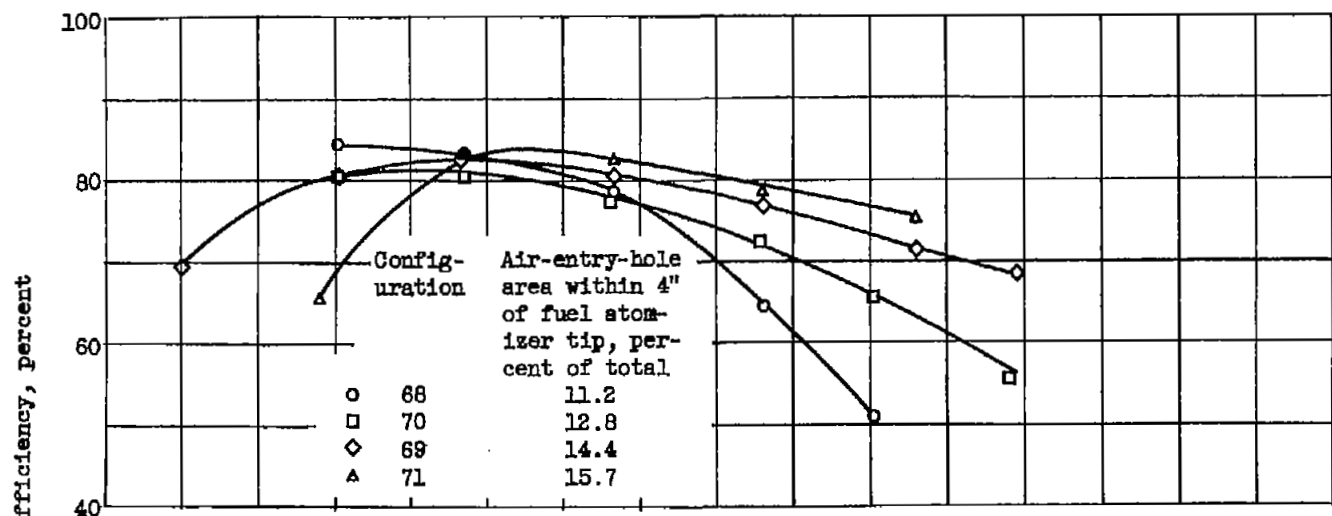
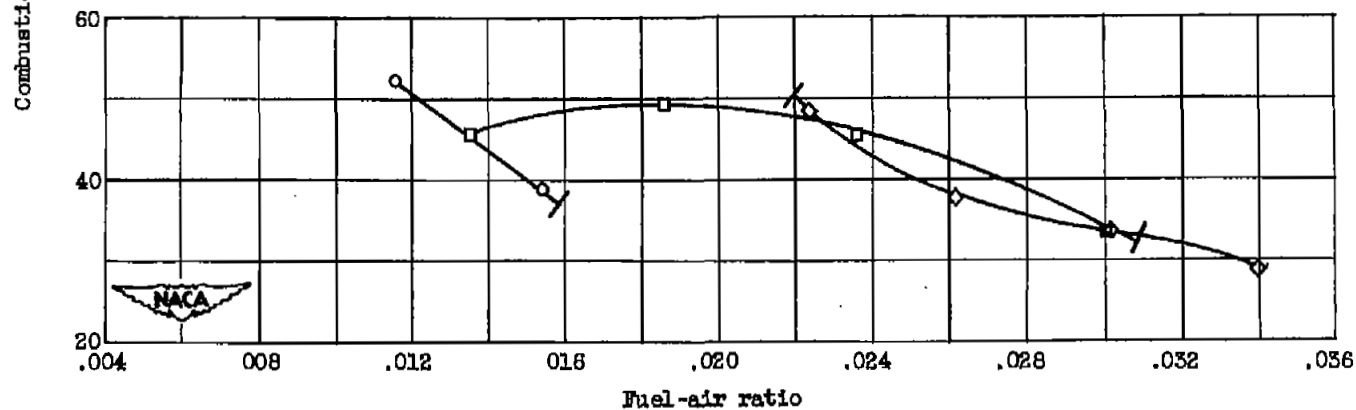


Figure 15. - Combustor-outlet gas-temperature profiles at condition B for funneled-, segmented-, and zigzag-flow configurations.



(a) Operating condition C.



(b) Operating condition D.

Figure 16. - Effect of variation in percent total air-entry-hole area within 4 inches of plane of fuel atomizer tip on combustion efficiency at two operating conditions.

SECURITY INFORMATION



3 1176 01435 2661

